Coprolites of Late Triassic carnivorous vertebrates from Poland: an integrative approach

Michal Zatoń, Grzegorz Niedźwiedzki, Leszek Marynowski, Karim Benzerara, Christian Pott, Julie Cosmidis, Tomasz Krzykawski, Pawel Filipiak

Elsevier Editorial System(tm) for Palaeogeography, Palaeoclimatology, Palaeoecology
Manuscript Draft

Manuscript Number:

Title: Coprolites of Late Triassic carnivorous vertebrates from Poland: an integrative approach

Article Type: Research Paper

Keywords: Coprolites, vertebrates, carnivores, bacteria, biomarkers, Triassic

Corresponding Author: Dr. Michal Zaton, Ph.D.

Corresponding Author's Institution: University of Silesia

First Author: Michal Zaton, Ph.D.

Order of Authors: Michal Zaton, Ph.D.; Grzegorz Niedzwiedzki; Leszek Marynowski; Karim Benzerara; Christian Pott; Julie Cosmidis; Tomasz Krzykawski; Pawel Filipiak

Abstract: Vertebrate coprolites derived from the Upper Triassic terrestrial deposits of southern Poland have been subjected for various analytical methods in order to retrieve the information about their composition, potential producer's diet and nature of the preserved microbial structures. Morphologically, they have been classified to four morphotypes, of which only three were further analysed due to their good state of preservation. Their groundmass occurred to be composed by francolite, a carbonate-rich apatite, in which abundant coccoid structures are preserved. Based on various microscopic and organic geochemical techniques, they are interpreted as fossilized bacteria which could have mediated the phosphatization of the faeces. The thin sectioning revealed that the coprolites consist of those containing exclusively bone remains, and those preserving both bone and plant remains. Those coprolites preserving only vertebrate remains are suggestive for exclusive carnivorous diet of the producers. However, the interpretation of coprolites consisting of both vertebrate and plant remains is more debatable. Although they may attest for omnivory, it is not excluded that potential producers were carnivorous which occasionally ingested plants, or accidentally swallowed plant material during feeding. The latter may involve predation or scavenging upon other herbivorous animals which used to fed on plants. It is not excluded that the potential producers may have been animals that foraged in or near aquatic habitats, such as semi-aquatic archosaurs and/or temnospondyls, what is supported by the presence of ostracode remain and fish scales within the coprolites, as well as by the presence of such specific biomarkers as phytanic and pristanic acids, which are characteristic constituents of fish oil. The preservation of such labile organic compounds as sterols, palmitin, stearin or levoglucosan attests for mineralization of the faeces on very early stages of diagenesis.

Suggested Reviewers: Karen Chin
University of Colorado
karen.chin@colorado.edu
a renown specialist on coprolites

Matts Eriksson
Lund University, Sweden
mats.eriksson@geol.lu.se
a specialist who worked on Mesozoic coprolites

Ashu Khosla
Panjab University, India
khosla100@yahoo.co.in
a researcher who recently described similar to ours phosphatic coprolites full of plant remains

Jesper Milan
University of Copenhagen, Denmark
jesperm@oesm.dk
specialist on carnivoran coprolites

Jochen Brocks
The Australian National University
jochen.brocks@anu.edu.au
a specialist of biomarkers which were also investigated for the present paper

Michał Zatoń, Ph.D., D.Sc.
University of Silesia
Faculty of Earth Sciences
Będzińska 60
PL-41-200 Sosnowiec
POLAND
e-mail: mzaton@wnoz.us.edu.pl

To the Editor-in-Chief of the journal *Palaeogeography, Palaeoclimatology, Palaeoecology*

Dear Professor Bottjer,

We would like to submit the manuscript entitled "**Coprolites of Late Triassic carnivorous vertebrates from Poland: an integrative approach**" by Michał Zatoń, Grzegorz Niedźwiedzki, Leszek Marynowski, Karim Benzerara, Christian Pott, Julie Cosmidis, Tomasz Krzykawski & Paweł Filipiak to the journal *Palaeogeography, Palaeoclimatology, Palaeoecology*. The article is original and hasn't been submitted to any other journal before.

The article concerns the study of coprolites derived from the Upper Triassic, bone-bearing deposits of southern Poland. For the first time we used integrative approach combining various analytical methods (transmission-light microscopy, scanning electron microscopy, transmission electron microscopy, scanning transmission x-ray microscopy, X-ray absorption near edge structure, electron microprobe analysis, XRD, inorganic and organic geochemistry, palynology) in order to decipher various problems concerning the coprolites, including the coprolite composition, the producers' diet, the nature of the coprolite groundmass and microbial consortia preserved. Thus, to our knowledge, this paper is the first of such a kind ever published and may be a reference article to other research concerning paleobiology of coprolites. As recently the journal published several papers concerning coprolites and related papers, we think that the submitted article fits well the journal scope and would also be often cited in the future. Therefore, we hope the paper will be considered for the review process by the Editor.

As the potential referees, we would like to propose the following specialists in that matter:

1. Karen Chin, e-mail: karen.chin@colorado.edu, a renown specialist on coprolites
2. Matts Eriksson, e-mail: mats.eriksson@geol.lu.se, a specialist who worked on Mesozoic coprolites
3. Ashu Khosla, e-mail: khosla100@yahoo.co.in, a researcher who recently described similar to ours phosphatic coprolites full of plant remains
4. Jesper Milan, e-mail: jesperm@oesm.dk, another specialist on coprolites
5. Jochen Brocks, e-mail: jochen.brocks@anu.edu.au, a specialist of biomarkers which were also investigated for the present paper

Sincerely Yours,
On behalf of the co-authors
Michał Zatoń

Highlights

- Vertebrate coprolites from the Upper Triassic of Poland have been studied
- Phosphatic groundmass attests for carnivores as coprolite producers
- Groundmass is composed of coccoid structures interpreted as fossilized bacteria
- Carnivores incidentally/accidentally swallowed plants as evidenced from inclusions
- Preservation of many labile organic compounds indicates rapid faeces mineralization

Coprolites of Late Triassic carnivorous vertebrates from Poland: an integrative approach

Michał Zatoń[1*], Grzegorz Niedźwiedzki[2], Leszek Marynowski[1], Karim Benzerara[3], Christian Pott[4], Julie Cosmidis[5], Tomasz Krzykawski[1] and Paweł Filipiak[1]

[1]University of Silesia, Faculty of Earth Sciences, Będzińska 60, PL-41-200 Sosnowiec, Poland.

[2]Department of Organismal Biology, Evolutionary Biology Center, Uppsala University, Norbyvägen 18A, 752 36 Uppsala, Sweden.

[3]Institut de Minéralogie, de Physique des Matériaux, et de Cosmochimie, Sorbonne Universités – UPMC, CNRS & MNHN, 4 Place Jussieu, Paris, 75005, France.

[4]Department of Palaeobiology, Swedish Museum of Natural History, Box 50007, 104 05 Stockholm, Sweden.

[5]Department of Geological Sciences, University of Colorado, 2200 Colorado Avenue, Boulder, CO 80309.

[*]Corresponding author. E-mail: mzaton@wnoz.us.edu.pl (M. Zatoń).

Abstract

Vertebrate coprolites derived from the Upper Triassic terrestrial deposits of southern Poland have been subjected for various analytical methods in order to retrieve the information about their composition, potential producer's diet and nature of the preserved microbial structures. Morphologically, they have been classified to four morphotypes, of which only three were further analysed due to their good state of preservation. Their groundmass occurred to be composed by francolite, a carbonate-rich apatite, in which abundant coccoid structures are preserved. Based on various microscopic and organic geochemical techniques, they are interpreted as fossilized bacteria which could have mediated the phosphatization of the faeces. The thin sectioning revealed that the coprolites consist of those containing exclusively bone remains, and those preserving both bone and plant remains. Those coprolites preserving only vertebrate remains are suggestive for exclusive carnivorous diet of the producers. However, the interpretation of coprolites consisting of both vertebrate and plant remains is more debatable. Although they may attest for omnivory, it is not excluded that potential producers were carnivorous which occasionally ingested plants, or accidentally swallowed plant material during feeding. The latter may involve predation or scavenging upon other herbivorous animals which used to fed on plants. It is not excluded that the potential producers may have been animals that foraged in or near aquatic habitats, such as semi-aquatic archosaurs and/or temnospondyls, what is supported by the presence of ostracode remain and fish scales within the coprolites, as well as by the presence of such specific biomarkers as phytanic and pristanic acids, which are characteristic constituents of fish oil. The preservation of such labile organic compounds as sterols, palmitin, stearin or levoglucosan attests for mineralization of the faeces on very early stages of diagenesis.

Key words: Coprolites, vertebrates, carnivores, bacteria, biomarkers, Triassic

1. Introduction

Coprolites are fossilized faeces preserved in sedimentary rocks throughout the Phanerozoic. Treated as trace fossils (e.g., Hunt and Lucas, 2005a, b; Hunt et al., 1998, 2007), they are known from both terrestrial (e.g., Mancuso et al., 2004; Northwood, 2005; Smith and Botha-Brink, 2011; Owocki et al., 2012; Fiorelli et al., 2013; Bajdek et al., 2014; Khosla et al., 2015) and marine settings (e.g., Eriksson et al., 2011; Zatoń and Rakociński, 2014; Shen et al., 2014; Nakajima and Izumi, 2014). Although they are indirect traces of the potential producers, coprolites serve as a valuable source of information on the diet and physiology of extinct animals (e.g., Chin and Kirkland, 1998; Hollocher et al., 2005; Chin, 2007; Gill et al., 2009; Smith and Botha-Brink, 2011; Bajdek et al., 2014; Khosla et al., 2015), trophic chain structure and predator-prey interactions in the fossil record (e.g., Chin, 2002; Northwood, 2005; Aldridge et al., 2006; Zatoń and Rakociński, 2014; Nakajima and Izumi, 2014). Moreover, as lithified structures, they also provide important data on sedimentary environments and early diagenetic processes leading to their formation, as well as on microbial and invertebrate communities operating within the faeces during their residence in the given palaeoenvironmental setting (e.g., Lamboy et al., 1994; Hollocher et al., 2001, 2005, 2010; Chin et al., 2009; Eriksson et al. 2011; Owocki et al., 2012; Mahaney et al., 2013; Cosmidis et al., 2013).

Even though coprolites are not directly associated with their producers, several indicators are used to decipher the potential culprits. Coprolite size, shape and fossil content (inclusions) may depend on whether the producer was invertebrate or vertebrate, and whether it was an herbivore, omnivore, insectivore or carnivore animal (e.g., Chin and Kirkland, 1998; Chin et al., 1998; Edwards et al., 2012; Wood and Wilmshurst, 2014; Khosla et al., 2015). Moreover, on the basis of the degree of food degradation or preservation of specific biomarkers, the kind of metabolism of a producer may also be untangled (e.g. Gill et al., 2009, 2010; Owocki et al., 2012). All these data, together with information on animal fossils preserved in the same deposits may provide a quite

coherent knowledge on the nature of possible producers. Sometimes, in very favourable diagenetic microenvironments, the food remains may be exceptionally well-preserved, providing additional coprolite 'taphonomic windows' into past life and victim identity (e.g., Meng and Wyss, 1997; Chin et al., 2003; Northwood, 2005; Yates et al., 2012; Dentzien-Dias et al., 2013; Zatoń and Rakociński, 2014).

In the present work, we focus on Late Triassic phosphatic coprolites derived from terrestrial palaeoenvironments of the southern territories of Poland, where a number of different vertebrate assemblages were discovered in recent times (Dzik and Sulej, 2007; Dzik et al., 2008; Budziszewska-Karwowska et al., 2010; Sulej et al., 2011, 2012; Niedźwiedzki et al., 2012, 2014). The late Triassic was a critical moment in the evolution of land vertebrates (e.g., Sues and Fraser, 2010; Brusatte et al., 2010). During those times, important groups of tetrapods, such as crocodiles, pterosaurs, dinosaurs and mammals, evolved to flourish later on in the Mesozoic era. Therefore, the coprolites from that period are important data documenting the source of diet, interactions, as well as local community structures. Recently, plant-rich putative coprolites produced by dicynodonts have been described from the Late Triassic deposits of southern Poland by Bajdek et al. (2014). In the present paper, we focus on carnivore coprolites studied by various analytical methods in order to retrieve the information about their geochemical composition, the diet of potential producers and preserved microbial structures.

2. Geology, stratigraphy and palaeocommunity structure

The latest Triassic (late Norian-Rhaetian) was an interval of abrupt evolutionary changes in terrestrial ecosystems (Sues and Fraser, 2010). The end of the Rhaetian was evidently also a time of widespread igneous activity in the rift basins of the Atlantic margins (e.g., Schoene et al., 2010) and extinction of many typical Triassic groups of land tetrapods (e.g., Olsen et al., 2002). The record of this extinction event is also visible in the Triassic of Poland (Pieńkowski et al., 2014). In the Late

Triassic times, the Silesia area (southern Poland) was located at the western margin of a large Laurasian landmass, at approximately 40° N palaeo-latitude and was the part of the north-east margin of the Germanic Basin (Golonka, 2007). This part of the basin is still poorly understood and contains floristic and faunal elements unknown from other areas of the Germanic Basin (e.g. Dzik and Sulej, 2007; Dzik et al., 2008; Niedźwiedzki et al., 2014).

Figure 1 near here

2.1. Poręba site

A short overview of the geology and stratigraphy of the Poręba site was recently presented by Sulej et al. (2012) and Niedźwiedzki et al. (2014). The site is located in the northern part of Poręba city, about four kilometres from Zawiercie, southern Poland (Fig. 1). The strata exposed at Poręba belong to the upper part of the Middle Keuper sequence in southern Poland. In the Polish lithostratigraphic scheme (see Polish Stratigraphical Table, 2008), they are referred to as the Zbąszynek beds (Woźniki Limestone or Woźniki Formation in local lithostratigraphical schemes; see Szulc et al., 2006). The Zbąszynek beds exposed at Poręba contain conglomerates (with rare magmatic rocks and quartzitic pebbles), grey to yellowish sandstones, grey to greenish mudstone and siltstone, ‘bone-breccia’ horizons (horizons termed as the ‘Lisów Breccia’ by geologists) and horizons with carbonaceous nodules (probably pedogenic in origin), as well as pyrite nests (Fig. 2). The Zbąszynek beds are correlated with the upper part of the Middle Keuper–lowermost part of the Upper Keuper formations (middle–upper Stubensandstein-Steinmergelkeuper or upper Arnstadt Formation and lowermost Exter Formation) from the Germanic Basin (see Franz et al., 2007a, b; Franz, 2008). This lithostratigraphic position of the Poręba exposures is essentially equivalent to that of mid–upper Middle Keuper strata detected in the Niwki and Poręba boreholes, both located close to the fossil-bearing site (Szulc et al., 2006).

The coprolite-bearing strata exposed at Poręba are yellowish, bone-rich, carbonated conglomerates, bone-breccia and grey fluvial carbonitic, organic-rich mudstones and siltstones with large fragments of fossil wood (trunks fragments), charcoals (Marynowski et al., 2014), bivalves, ostracods, conchostracans, plant remains, plant roots, microbial oncoids and small carbonate nodules. The entire observed stratigraphic section in this locality is at least 8 m thick and contains four distinct horizons (a-d) with vertebrate bones (Fig. 2).

Figure 2 near here

Palynological studies suggest a middle–late Norian age for the Poręba site (Niedźwiedzki et al., 2014). More than 50 palynomorphs were identified in one organic-rich sample from the layer located above the uppermost bone bed. This palynoassemblage is characteristic for subzone b of the *Corollina meyeriani* Zone (see Orłowska-Zwolińska, 1983, 1985) in the Polish part of the Germanic Basin and is characteristic of the lower–middle part of the Zbąszynek beds and the underlying Jarkowo beds. The subzone IVb of the *Corollina meyeriana* Zone probably corresponds to the *Corollina-Porcellispora* Subzone, the lower part of the *Corollina-Enzonalasporites* Zone of Lund (1977), zones GTr 16–17 of Heunisch (1999) and the *Granuloperculatipollis rudis* Zone of Kürschner and Herngreen (2010). The IVb Subzone assemblages are similar to those of the Steinmergelkeuper (Orłowska-Zwolińska, 1985).

The tetrapod record in Poręba (Fig. 3) is dominated by skeletal remains of turtles, which are represented mainly as isolated plates (or fragments of plates) from carapace or plastron, vertebrae and fragments of long bones (Sulej et al., 2012). These remains represent possibly a single species of terrestrial turtle, which is a new taxon similar to *Proterochersis robusta*. Several isolated dinosauriform specimens were collected from Poręba (Niedźwiedzki et al., 2014). This assemblage includes a silesaurid, specimens of herrerasaurid, and remains of another type of theropod (potentially a neotheropod). The Poręba herrerasaurid is the first record of this rare group of

primitive saurischia or basal theropod from Europe and one of the youngest records worldwide, whereas the silesaurid is the youngest record from Europe. Other vertebrate remains are rare, but include vertebra and dermal elements of aetosaurs, dipnoan teeth plates, hybodont shark fin spines and teeth, as well as actinopterygian fish skull elements and scales. Preserved fragments of bones and teeth of a large carnivorous archosaur (possibly a 'rauisuchian' or a mid-sized theropod dinosaur) were also found in this locality. A few isolated teeth and a small part of the shaft of a large long bone collected from the organic-rich mudstone and claystone intervals belong to large temnospondyls.

Besides the mentioned and in part published material, there are still many undescribed plant macrofossils, unrecognizable bones and a collection of bivalves. The plant fossils in the Poręba outcrop are very abundant and well preserved, but not characterized in details. The dominant plant species is a conifer similar to *Brachyphyllum*. Fragments of branches with leaves and numerous fragments of charcoalified or mineralized wood trunks, sometimes of large size, also occur in the organic-rich mudstone and claystone (Sulej et al. 2012). *Brachyphyllum* is characterized by xeromorphic leaves and pollen cones, which suggests a drier/sunny habitat or a dry season during this time. More than 25 species of palynomorphs were identified in one organic-rich sample (Niedźwiedzki et al., 2014). This palynoassemblage contains spores and pollen grains belonging mainly to gymnosperms and ferns.

The Poręba fossil assemblage, as currently known, is composed of more than six tetrapod taxa. More than half of the collected fossils are represented by the new taxon of turtles. This taxon was arguably one of the most abundant animals inhabiting the Poręba ecosystem. Another remarkable aspect of the assemblage is the great diversity of the dinosauriforms, which is greater than that of the other archosauromorphs combined. Large aquatic archosauromorph taxa such as phytosaurs and large dicynodonts, which are typical elements of the Late Triassic freshwater ecosystems are conspicuously absent from the assemblage.

Figure 3 near here

2.2. Lisowice site (Lipie Śląskie clay-pit)

According to Dzik et al. (2008), Niedźwiedzki et al. (2012), Pieńkowski et al. (2014) and Niedźwiedzki (2015), strata exposed in the Lipie Śląskie clay-pit at Lisowice (Fig. 1) correspond to the uppermost part of the Middle and lower part of the Upper Keuper deposits of the Germanic Basin (see also Franz et al., 2007a, b; Franz, 2008). In the geological literature, the lithostratigraphic unit represented at the Lipie Śląskie clay-pit (Fig. 4) has been referred to as Norian (see Szulc *et al*. 2006) or Rhaetian "*sensu polonico"* (see Franz et al., 2007a, b; Franz, 2008).

The identification of a palynomorph assemblage, which represent the Subzone IVc of the *Corollina meyeriana* and *Ricciisporites tuberculatus* zones, with characteristic forms such as *Rhaetipollis germanicus* Schulz, *Ricciisporites tuberculatus* Lundblad, *Corollina meyeriana* (Klaus) Venkatachala *et* Góczán, *Granuloperculatipollis rudis* Venkatachala *et* Góczán (see Świło et al., 2014) in the dark-grey and organic-rich strata at the Lipie Śląskie clay-pit suggest correlation of this unit with the uppermost Zbąszynek beds and lower Wielichowo beds (uppermost Norian-lower Rhaetian) from the northern part of Poland (Orłowska-Zwolińska, 1983; Franz, 2008).

The Lipie Śląskie clay-pit at Lisowice contains a larger number of fossils (Fig. 5) than the Poręba exposure and it is one of the most diverse vertebrate assemblages of Late Triassic age in Poland, representing up to 15 taxa (Niedźwiedzki, 2015). Most of the vertebrates occur in the grey carbonate mudstones and siltstones in the middle part and at the top of the exposed section (Fig. 4). The vertebrate assemblage is dominated by bones of a gigantic dicynodont and isolated remains of actinopterygian fishes. Other vertebrate skeletal remains are represented by a small archosauromorph, a large capitosaur, and a small plagiosaur. The Lisowice fauna is dominated by terrestrial rather than amphibious or aquatic tetrapods. In two layers with large jet-like wood fragments, remains of dicynodonts are associated with remains of *Smok wawelski* (an early

predatory dinosaur), small to medium-size archosaurs (pterosaur, dinosauriform, small predatory dinosaur and poposaurid), and other non-archosaur archosauromorphs (e.g. a choristodere-like animal) and small diapsids. Identification of many of the disarticulated, often fragmentary bones of other tetrapods is difficult and usually problematic (Dzik et al., 2008; Niedźwiedzki et al., 2012; Niedźwiedzki, 2015). The temnospondyls (*Cyclotosaurus* sp. and *Gerrothorax* sp.) are known from an isolated, partially preserved skull, skull bones, jaw bones, and numerous long bones collected in a layer less than one meter above the principal bone-bearing bed of the clay-pit exposure. A few isolated long bones of capitosaurs and plagiosaurs were also found in the main bone-bearing horizon. Such 'amphibian assemblages' are typical of a frequently flooded alluvial floodplain. Numerous macroremains of coelacanth and dipnoan fishes and spines of hybodont sharks (Świło, 2010a, b, c; Świło and Kowalski, 2011) were also found. A very rare mammaliaform or mammal teeth (Morganucodontidae indet.) were also recorded (e.g., Świło et al., 2014).

Figure 4 near here

The mudstone and siltstone intervals contained a rich assemblage of ostracods, conchostracans, bivalves, and rare insect remains (Dzik et al., 2008; Kozur and Weems, 2010; Skawina and Dzik, 2011). The most common are ostracods (*Darwinula* sp. and *Rhombocythere* sp.) and occur only in few horizons and, if present, form massive accumulations. The conchostracans *Gregoriusella polonica* Kozur *et* Weems, 2010 and *Euestheria* sp. of a very small size (1.5-3.5 mm in length) are rare and occur in two horizons in association with small vertebrate bones. In the lowermost part of the grey unit, numerous carapaces of much larger species *Shipingia* sp. (3-6 mm in length) were collected. Numerous bivalves collected from the mudstone facies strata represent the large unionoid *Tihkia silesiaca* Skawina *et* Dzik, 2011. Insect remains are very rare in this site. Until now only five specimens of isolated beetle elytra were collected from grey mudstone and siltstone of the lower part of bone-bearing deposits.

In the bone-bearing strata, numerous well-preserved macrofloral remains were found (Staneczko, 2007; Dzik et al., 2008; Wawrzyniak, 2010a, b, c, 2011; Wawrzyniak and Ziaja, 2009). The dominant plant species in this site is a conifer similar to species of the genera *Brachyphyllum*, *Pagiophyllum* or *Hirmeriella*, but other plants, probably representing the cycadophytes *Nilssonia* and *Beania* are also present (Wawrzyniak, 2010a). Other plant fossils are represented by representatives of cycadophytes, ginkgophytes, coniferophytes or pteridosperms, among which isolated cuticles of *Lepidopteris ottonis*, confirming the Rhaetian age of the plant beds occur (Staneczko, 2007; Ociepa et al., 2008; Wawrzyniak, 2010a, 2011; Pacyna, 2014).

The Poręba and Lisowice sites contain two distinct and different faunas, supposedly with only a few overlapping vertebrate taxa (Figs. 3, 5). The Poręba tetrapod fauna is dominated in numbers by dinosauriforms (Silesauridae and basal theropods or saurischia) with turtles, aetosaurs and temnospondyls as additional elements. The Lisowice site contains a record of gigantic dicynodont and large early predatory dinosaur. Temnospondyl remains are relatively abundant in the Lisowice fauna and are represented by two or even three species. The small reptilian diversity is relatively high as indicated by pterosaur, dinosauriform, small predatory dinosaur, poposaurids, choristodere-like animal and other small diapsids (Niedźwiedzki, 2015). Moreover, the presence of basal mammaliaform or early mammal in the Lisowice fauna further points to the different nature of both faunas (Świło et al., 2014).

Figure 5 near here

3. Material and methods

In total, 39 specimens have been collected for the present study. However, due to the overall state of preservation, only 18 coprolites have been considered for the present study (Table 1). Sixteen coprolites were collected in Lisowice from siltstones and mudstones, relatively rich in

organic remains (reaching up to 2.5% TOC; Marynowski and Wyszomirski, 2008), which represent low-energy environments, and two specimens were collected in the Poręba site within a conglomerate layer deposited in a high energy environment; probably it represents stream deposit. For the present study, a wide array of methods and analytical techniques has been used in order to retrieve the information about coprolite composition, diet of potential producers, palaeoenvironment and diagenesis. The raw samples are housed at the Institute of Paleobiology, Polish Academy of Sciences, Warsaw, abbreviated ZPAL V.39/372 (for Poręba) and ZPAL V.33/1270 (for Lisowice). The thin sections, as well as residues from palynological preparations are deposited at the Faculty of Earth Sciences, University of Silesia, Sosnowiec, abbreviated GIUS 7-3653.

Table 1 near here

3.1. Inorganic geochemistry and X-ray diffraction (XRD)

For bulk geochemical data, nine coprolite samples and an additional one (enclosing sediment, COP04b) have been analysed using fusion-inductively coupled plasma (FUS-ICP) at the Actlab laboratory in Canada. For bulk mineralogical data, nine coprolites and one sample of enclosing sediment (COP04b) were analysed with an PANalytical X' Pert Pro MPD-PW 3040/60 X-ray diffractometer housed at the Faculty of Earth Sciences, Sosnowiec, Poland. The samples were grounded manually using an agate mortar for c. 5 min. A standard metal sample holder in the X'Pert Pro systems was filled with powder. To calibrate the peak line position, the following internal standard was used: Respirable α-Quartz for Quantitative XRD, Standard Reference Material, NIST, 1878a. XRD data were collected using the diffractometer equipped with a Theta-Theta geometry and X'Celerator – 1D silicon strip detector. Generator settings were 45kV and 30mA. All X-ray diffraction experiments were performed using a CoK_{α} radiation (λ=1,78901Å) and a Fe-filter to reduce the K_{β} radiation. Data were collected in the range of 3-75°2Θ with a

0.01°2Θ step size and 300sec counting time. The interpretation and quantitative analysis of the collected data were carried out by means of the HighScore+ Software using the ICSD database, version 2007. The quantitative content was calculated using the Rietveld Method. Reference carbonate-apatite patterns of Perdikatsis (1991) were used as a starting model for the refinement. The CO_3^{2-} content of carbonate-fluorapatite was determined from measurements of the Δ2Θ for the 004-410 reflections pair. The relationship given by Schuffert et al. (1990) was used for our calculations: $y= 10.643 \cdot x^2 - 52.512x + 56.986$, where y is the CO_3^{2-} amount [wt%] and x = Δ2Θ (004-410). The HighScore+ profile fit algorithm was used to determine the exact position of the 004 and 410 reflection. Shape parameter of the Pseudo-Voigt profile function and the background was refined.

3.2. Electron microprobe (EMP) analysis

Apatite analyses (major/minor elements) were carried out on one sample (COP04a) in the Inter-Institution Laboratory of Microanalyses of Minerals and Synthetic Substances, Warsaw, Poland, using a CAMECA SX-100 electron microprobe (15 kV, 20 nA). The apatite analyses have been normalized to the sum of 50 negative charges including 24 oxygen ions and two monovalent anions (fluorine site) according to the ideal chemical formula of apatite: $A_{10}(BO_4)_6(X)_2$, where the A site is occupied by Ca, Fe, Mn, Mg, Th, REE, Y and Na. The B site is occupied by P (substituted by S, Si) and the X site by F, Cl and OH^- ions. The hydroxyl content was calculated by normalization assuming ideal stoichiometry (i.e., no vacancies in the X site so that $F+CI+OH^- = 2$).

3.3. Total organic carbon (TOC) and total sulphur (TS) determination

Abundances of total carbon (TC), total inorganic carbon (TIC) and total sulphur (TS) were performed for eight coprolite samples using an Eltra CS-500 IR-analyzer with a TIC module at the Faculty of Earth Sciences, Sosnowiec, Poland. TC, TS and TIC contents were measured using an infrared cell detector of CO_2 and SO_2 gas, which was evolved by combustion under an oxygen

atmosphere for TC and TS respectively, and was obtained from reaction with 10% hydrochloric acid for TIC. Total organic carbon (TOC) was calculated as the difference between TC and TIC. Calibration was made by means of Eltra standards. Calcium carbonate content was calculated as $CaCO_3$ = 8.333 x TIC, assuming that all carbonate is present as calcite.

3.4. Extraction, separation and derivatization.

Six finely ground coprolite samples were extracted under 60°C and 150 bars using DCM / methanol mixture (5:1, v:v) with an accelerated solvent extractor Dionex ASE 350. Extracts were separated into aliphatic, aromatic and polar fractions by modified column chromatography (Bastow et al., 2007). Silica-gel was first activated at 110°C for 24 h and then put into Pasteur pipettes. The eluents for collection of the fractions were: *n*-pentane (aliphatic), *n*-pentane and DCM (7:3 - aromatic), and DCM and methanol (1:1 - polar). An aliquot of the polar fraction was converted to the trimethylsilyl (TMS) derivatives by reaction with *N,O*-bis-(trimethylsilyl)trifluoroacetamide (BSTFA) and pyridine for 3 h at 70 °C. A blank sample was analysed using the same procedure. In the blank sample, trace amounts of phthalates, fatty acids (FAs) and *n*-alkanols were detected.

3.5. Gas chromatography – mass spectrometry (GC-MS).

The GC-MS analyses were carried out with an Agilent Technologies 7890A gas chromatograph and Agilent 5975C Network mass spectrometer with Triple-Axis Detector at the Faculty of Earth Sciences, Sosnowiec, Poland. The J&W DB35-MS (60 m × 0.25 mm × 0.25 μm) capillary column with 35% polymethylsiloxane and 65% diphenylsiloxane was used. The GC was programmed from 50°C after 1 min to 120°C at 20°C/min, and then to 300°C at 3°C/min, with final temperature maintained for 90 min. The GC column outlet was connected directly to the ion source of the mass spectrometer. Mass spectra were recorded from *m/z* 45–550 (0–40 min) and *m/z* 50–700 (above 40 min). The MS was operated in the electron impact mode (ionization energy 70 eV). An

Agilent Technologies Enhanced ChemStation (G1701CA ver. C.00.00) and the Wiley Registry of Mass Spectral Data (8th edition) software were used for data collection and MS processing.

3.6. Thin sections.

In order to retrieve the information about fossil inclusions and petrography, 15 samples, including two possible pyritized coprolites, have been sectioned longitudinally and transversely to the longest axis at the Faculty of Earth Sciences, Sosnowiec, Poland. Thin sections were then inspected using an Olympus transmitted light microscope and a Philips XL30 environmental scanning electron microscope (ESEM) at the Faculty of Earth Sciences, Sosnowiec, Poland.

3.7. Investigation of the coccoid structures.

In order to check and verify the nature of the coccoid structures present in the coprolites, one coprolite sample (COP04a) was further analysed by scanning electron microscopy (SEM), transmission electron microscopy (TEM) and scanning transmission x-ray microscopy (STXM).

General SEM observations were conducted at the Faculty of Earth Sciences, University of Silesia, Sosnowiec, using an ESEM Philips XL 30. The samples were investigated in uncoated state using back-scattered imaging (BSE). The detailed investigations were performed at the Institut de Minéralogie, de Physique des Matériaux et de Cosmochimie, Paris, France, using a Zeiss Ultra 55 SEM equipped with a field emission gun. COP04a was freshly broken and polished using Al_2O_3. The surface was then platinum-coated. Images were acquired with the microscope operating at 15 kV, and a working distance of 7.5 mm in secondary electron mode using the SE2 detector, or in backscattered electron mode using the AsB detector. Energy dispersive x-ray spectrometry (EDXS) analyses were performed at 15 kV at a working distance of 7.5 mm using a Bruker Quantax spectrometer.

For TEM and STXM analyses, two electron- and x-ray-transparent foils were prepared. The foils were extracted by focused ion beam (FIB) milling from the non-embedded polished COP04a

sample using a FEI strata DualBeam 235 FIB at the Institut d'Electronique, de Microelectronique et de Nanotechnologies (IEMN), Lille, France. The FIB foils were lifted out and welded on one side onto a copper grid (without carbon membrane) *in situ* before final polishing. The final foils measured ~18 μm long, ~8 μm wide and 100-200 nm in thickness for FIB foil#1 and ~22 μm long, ~12 μm wide and 100-200 nm in thickness for FIB foil #2. Rationale for the use of FIB milling and recent applications in geobiology can be found in Benzerara et al. (2005) and Bernard et al. (2010).

The FIB foils were first analysed by STXM at the carbon K-edge and the Ca $L_{2,3}$-edges. STXM and X-ray absorption near edge structure (XANES) analyses were performed on beamline 11.0.2.2. at the Advanced Light Source (Lawrence Berkeley National Laboratory, Berkeley, USA) (Bluhm et al., 2006). Energy calibration was achieved using the well-resolved 3p Rydberg peak of gaseous CO2 at 294.96 eV (Ma et al., 1991). A 25 nm zone plate was used. Data included images and image stacks, from which XANES spectra and maps were retrieved. Data were processed using the aXis2000 software (Hitchcock, 2012). Rationale for the use of STXM to study biominerals, including Ca-phosphates can be found in Benzerara et al. (2004) and Cosmidis and Benzerara (2014).

FIB foils were then analysed by TEM. Observations were performed on a LaB6 JEOL JEM 2100 TEM operating at 200 kV. Images were acquired using an ultrascan 2k CCD camera in bright field mode. Compositional maps were acquired by EDXS analysis in the STEM mode.

3.8. Preparation of palynomorphs and other organic remains.

In order to better recognize the organic remains, ten samples were selected for palynological investigation. Generally, c. 10 g of each coprolite were processed using standard palynological procedures HCl-HF-HCl (Wood et al., 1996). Finally, residues were sieved through an 18 μm nylon sieve. Four slides were prepared from each residue. Generally, the organic remains were segregated into six categories: miospores (pollen grains and spores), higher plant cuticles, higher plant tracheids, translucent organic particles, black organic particles and animal remains (mostly

cuticles). Then, the cuticles were identified to the lowest possible taxonomic level. Two hundred palynomorphs were counted for each coprolite sample for statistical purpose. The observation and documentation was completed using a transmitted light microscope (Olympus BX51 with DS-U3 controller and Nikon's NIS-Elements imaging software suite) and an ESEM Philips XL30. The palynological slides and residues are housed at the Faculty of Earth Sciences, Sosnowiec, Poland.

4. Results

4.1. Morphology, size and composition

Most of the coprolites collected were found as loose fragments on the surface of the freshly exposed deposits, but in some cases they were found *in situ* within the host rock. Many of the collected specimens are fragmentarily preserved or lack any distinctive features and thus are referred to as possible coprolites. They are also usually pyritized so that both their external morphology and primary composition is obliterated. Better or completely preserved specimens are represented by four distinct morphotypes.

Figure 6 near here

Morphotype 1 is represented by six specimens characterized by both ends similarly rounded (isopolar of Thulborn, 1991). Some of these coprolites are elongated, rod-like shaped (see Eriksson et al., 2011) with circular to semi-circular cross-section (Fig. 6B, D, G, J). They measure 53–160 mm in length and 16–70 mm in width. Others are ovoidal, measuring 46–73 mm in length and 18–25 mm in width. Detailed description of the largest and cylindrical coprolites (60-160 mm long) from the Lisowice site is presented by Niedźwiedzki (2015) and interpreted as faecal mass produced by the large early predatory dinosaur *Smok wawelski* (Niedźwiedzki et al., 2012; Niedźwiedzki, 2015).

Morphotype 2 comprises 14 coprolites having one end wider than the other (anisopolar of Thulborn, 1991). To that group belong those having a smooth exterior but having one end much narrower than the other or even pointed (Fig. 6A, C, F, H); other specimens of that morphotype are ovoidal with both ends differing, but not as much as the previous case (e.g., Fig. 6C, I). Two specimens have a distinct, circular cavities inside the wider ends (Fig. 6A, C). The coprolites are 14–45 mm in length and 7–46 mm in width.

Morphotype 3 includes ten coprolites with irregular (ellipsoidal to ovoidal) shapes. Eight specimens, however, are strongly pyritized and thus considered here as possible coprolites. They may be up to 100 mm in length (Fig. 6K).

Morphotype 4 contains nine, tiny, 9–32 mm long, thin and curved specimens. Due to their pyritization (Fig. 10D), they are considered as possible coprolites and were not furthered analysed. Two cylindrical specimens are a little bit flattened and are more regular in shape and surface morphology.

When viewed in cross-section, some coprolites show that they are composed of more or less visible concentric layers (Fig. 6J). The large scale coil deformations present in the studied specimens are features probably generated when the faecal material was squeezed along the producer's intestine and extruded from the cloaca. The mass of the coprolites is beige or brown in colour. Most of the coprolites have a sharp outer contact with a clear separation from the host sediment. The exterior surface of the coprolites is usually irregular, although it can be smooth in some cases. It is sometimes covered by adherent clay with carbonaceous matter and also sediment grains.

Table 2 near here

As evidenced from thin sections, the coprolites have a very fine-grained, micro-crystalline and apatitic groundmass. Bulk chemical analyses showed that the coprolites are primarily composed

of Ca and P with low amount of SiO_2. The phosphate content is variable and ranges from 9.1 wt. % to 20.3 wt. % (Table 2). The XRD analyses are in agreement, showing that the main minerals building the coprolites are apatite and calcite (Table 3). However, their mass percentages obtained by FUS-ICP and XRD may vary either due to measurement errors, and quite significant content of different elements in the apatite structure. Also the content of OH^--groups, as well as a porosity of the coprolites may result in such differences. Calcite and apatite are associated with admixture of other minerals such as quartz, pyrite and barite. Traces of clay minerals, iron oxides (goethite) and dolomite are also possible (Table 3).

Table 3 near here

Figure 7 near here

The XRD analyses showed that phosphate occurs in the form of francolite, a carbonate-rich variety of the mineral fluorapatite, which is consistent with EMP analysis and SEM-EDXS mapping. In the SEM backscattered electron mode, fragments of francolite (rich in Ca and P) appear in light grey in a matrix of Ca-carbonates, which appears in darker grey (Fig. 7).

Figure 8 near here

TEM-EDXS were also consistent with SEM analyses (Fig. 8). Francolite is composed of Ca and P in a ratio of ~1.6. Moreover, F, Na and S were systematically detected in association with francolite. As the XRD analysis showed, phosphate-rich coprolites clearly differ from the enclosing sediment (Fig. 9), which mainly contains quartz (45 wt. %) and calcite (40 wt. %); clay minerals are represented by dioctaedric smectite, kaolinite, chlorite and illite (Σ ~8 wt. %). Small admixtures of dolomite (~3 wt. %), feldspars (~3 wt. %) and pyrite (~1 wt. %) were also detected. Generally, the

composition of the coprolites, especially the presence of francolite and calcite, is similar to other described examples (e.g., Hollocher et al, 2005, 2010; Eriksson et al., 2011).

Figure 9 near here

Thin sections of the coprolites reveal fragmented bones and other animal or plant tissues. The coprofabric may either differ between particular coprolite morphotypes, or may be similar. For example, some coprolites of the morphotype 2 (e.g., samples COP01 and COP14) may possess characteristic mucosal folds (e.g., Jain, 1983; Eriksson et al., 2011), composed of very fine-grained apatitic mass, interfingered with sparry calcite (Fig. 10A-B), which do not occur in those of the morphotype 1 and 3. However, the coprofabric consisting of of micro-crystalline phosphatic groundmass (Fig. 10C) with some sparry calcite and pyrite grains, without any mucosal folds and large areas occupied by calcite crystals, may occur in morphotypes 1, 2 and 3. The pyritized putative coprolites instead, have completely obliterated coprofabric (Fig. 10D).

Figure 10 near here

4.2. Bulk and molecular composition of coprolites

The total organic carbon (TOC) content in coprolites varied significantly between 0.4 to 1.5% (Table 4). In almost all samples, very low concentrations of total sulphur were detected, which is characteristic for terrestrial sedimentary environments and organic matter (OM) originated from such deposits. One exception, where TS >1%, occurred in one sample that was showing secondary pyritization.

Table 4 near here

Coprolite samples were characterized by very similar molecular composition, with prominence of the polar fraction and a very low percent amount of aromatic compounds.

The aliphatic fraction was characterized by a preponderance of low-molecular weight *n*-alkanes with maximum in *n*-C_{17} and *n*-C_{18}. High molecular weight *n*-alkanes were present in low concentration but predominance of odd over even high-molecular weight *n*-alkanes was detected in most of the samples. The aliphatic fraction of coprolites contained series of mid-chain methyl-alkanes and cycloalkanes and two common isoprenoids: pristane and phytane, which were present in comparable amounts (Fig. 11). Low relative concentrations of ααα-steranes with small predomination of C_{27} over C_{29} compounds were detected in two samples (COP09 and COP18).

Figure 11 near here

Aromatic compounds were present in very low abundance in the samples. Only few compounds were identified including phenanthrene and its methyl- and dimethyl- derivatives, fluoranthene, pyrene and phenylnaphthalenes (1- and 2-PhN). Among aromatic nitrogen compounds, benzocarbazole isomers were identified.

In the polar fraction, homologue series of *n*-alkanoic acids and *n*-alkanols clearly dominated with preponderance of *n*-hexadecanoic acid (Table 5, Fig. 12). Even-carbon homologues predominated the distribution of *n*-alkanols, while in case of *n*-alkanoic acids such domination was clearly visible starting from $C_{15:0}$ fatty acids. Beside saturated *n*-alkanoic acids and *n*-alkanols, $C_{16:1}$ and $C_{18:1}$ fatty acids and alcohols were detected at high relative concentration (Table 5) in all coprolite samples. Sterols were a quantitatively significant group of compounds. More specifically, sitosterol was the main sterol compound and cholesterol was the second most important. Degradation products of sterols (cholesta-3,5-dien-7-one and stigmasta-3,5-dien-7-one) were also detected. Fats such as palmitin and stearin (both 1- and 2- glyceryl esters) were present in significant amount as well (Table 5, Figure 12). Other polars detected in coprolite samples as minor

compounds were isoprenoid acids (pristanic and phytanic acid), urea, levoglucosan and β- and α-amyrin (Table 5).

Table 5 near here

Figure 12 near here

4.3. Coccoid structures within apatite groundmass

The ESEM investigation of both broken coprolites and thin sections revealed that the apatitic groundmass (including mucosal folds) is composed of abundant spherical objects measuring up to 3 µm in diameter (Fig. 7). These structures, forming dense aggregations, were systematically observed in the francolite fragments of the coprolites (Fig. 8). Two 100-200 nm thick electron transparent foils were cut within these francolite fragments. TEM observations confirmed that francolite fragments are composed of packed micrometer-sized spheres. These spheres are outlined by a dense wall of francolite, ~120-150 nm thick. Some spheres appear as empty shells while other are filled by francolite laths measuring ~300 by ~50 nm wide and are radially elongate (Fig. 8). Hexagonal sections were occasionally observed, consistently with francolite habits.

STXM analyses were performed on the same foils at the C K-edge and the Ca $L_{2,3}$-edges. Spectra at the Ca $L_{2,3}$ edges were very similar all over the examined areas, suggesting that only one Ca-containing phase, i.e., francolite is detected on the FIB foils. Spectra showed major peaks at 349.3 and 352.6 eV which correspond to the L_3 and L_2 edges of Ca respectively, as well as smaller features at 347.2, 347.8, 348.3, 348.7 and 351.6 eV (Fig. 8I). Such spectra are typical of apatitic minerals including francolite (Benzerara et al., 2004). A prominent narrow peak was observed at 290.3 eV at the C K-edge as well as a broader peak at 300.9 eV (Fig. 8J). They are interpreted as $1s \rightarrow \pi^*$ and $1s \rightarrow \sigma^*$ electronic transitions in carbonates respectively. Based on the ratio between the height of the peak at 290.3eV and the edge step between 340 and 360 eV at the Ca $L_{2,3}$-edges, the CO_3 content of francolite was mapped using the approach developed by Cosmidis et al. (2014). The

ratio was relatively homogenous over the explored area and estimated between 4 and 6% of CO_3 in wt. Some organics was also detected as indicated by peaks at 285 eV, interpreted as 1s→π* in aromatic groups, and at 288.5 eV, interpreted as 1s→π* in carboxylic groups. Mapping showed that organic-rich areas appear on edges of the FIB foil and/or lining holes inside the spheres. TEM-EDXS analyses on the same areas showed a systematic enrichment in gallium (Fig. 8G). Although some organic carbon might be originally associated with these structures, areas rich in organic carbon are interpreted as re-deposition of contaminating carbon during FIB milling by the gallium beam. The origin of contaminating carbon might be, at least partly, contamination from the decomposition of the organometallic precursor used for platinum deposition, which is rich in aromatic groups (Carlut et al., 2010). This is consistent with the observation that re-deposition is higher where porosity is higher.

In some cases, spheres are completely filled by fine-grained francolite. In these cases, one or two concentric <100 nm wide, darker layers delimitated the spheres as observed in the TEM bright field mode (Fig. 8B). Since Ca, P, S, F and Na, as well as CO_3 groups as shown by TEM-EDXS and STXM analyses are all higher in these darker layers, they are interpreted as layers with less nano-porosity, hence higher density of francolite grains. As evidenced from the EMP analyses, the francolite containing the coccoid structures does not show zoning with respect to chemical composition (see ESM Fig. 1C).

4.4. Fossil inclusions and their preservation

Different inclusions were identified on the external surface of the specimens, as well as in the interior of broken samples. Most of the elements, however, were identified inside the coprolites using thin sections. They were embedded in a microcrystalline apatitic matrix and represent a variety of fossils, including bone fragments and scales (Figs 13-15), plant remains and palynomorphs (Figs 17-18), and arthropod cuticles (Fig. 19).

Figure 13 near here

4.4.1. Scales, teeth and bones

Nearly all identified bone fragments originated from small prey animals and were evenly scattered within the individual coprolites. In two coprolites, long fragments of dicynodont bones were identified (Niedźwiedzki, 2015), whereas in another one, a large isolated tooth of the large early predatory dinosaur *Smok wawelski* with sings of digestions was also found. Most of the bone fragments in the coprolites were white or brownish (Figs 13-15); the darker colour was due to humic acids produced by the biodegradation of the organic matter or mineral filling (e.g., pyrite or manganese oxides) the pores in observed bone elements. Some bone fragments showed external and internal damages such as deformed or missing tissues (e.g., Fig. 13E), suggesting pockets of decay. Cross-section of two specimens evidenced that most of the elongate bone fragments were oriented perpendicular to the long axis of the coprolite (e.g., Figs 13D, 15A).

Figure 14 near here

Two coprolites contained fish scales (Fig. 13F). The transverse section of one of the best preserved scale showed an amorphous, thick enamel layer, dentine with numerous dentinal tubules, Sharpey's fibers, and several lines of von Ebner (Fig. 13E). The scale was secondarily penetrated by straight and branching canals, probably of microbial (fungal?) origin. Several smaller unidentified bone fragments were also preserved (Figs 13A-C, 15A), including a fragment that was oval-shaped in cross-section; probably, it was a long bone of a small tetrapod with calcified cartilage of the bony trabeculae (Fig. 15C). In other coprolites, several sections of slowly forming and poorly vascularized bone (fish or amphibian bones) were also observed (e.g., Fig. 13A-B). The dentine of another preserved tooth fragment (Fig. 14C) showed dentinal tubules oriented perpendicularly to the pulp cavity. Enamel was preserved only in some margins of this tooth.

Different degrees of digestive corrosion of skeletal remains were observed in the coprolites. Some elements (e.g., scales) were complete in cross-section and others were represented by highly degraded bone fragments (Figs 14A-B, 15B). The coprolites also contained small bone splinters showing such signs of corrosion as markedly rounded and polished edges, suggesting rather strong digestive processes. Some bone fragments displayed characteristic fracture surfaces indicating breakage whilst the bone was still fresh (Fig. 13E). Part of the unidentified components may represent hard and mineralized bone elements. Some skeletal elements were perforated by tunnels, chambers and networks of microborings (Fig. 15C-F). This was the result of microbial attack (bacteria or fungi) of bony and probably collagen-rich elements after the faeces were excreted. One of the sectioned coprolite contains packed fibrous elements (Figs 14D, 15A). Whether they are digested remains of hairs is currently unclear as we didn't obtained any clear evidence using SEM. However, they are intriguing fossils the nature of which maybe is possible to decipher using other methods.

Figure 15 near here

The XRD data indicate, that the fossil bone fragments are similar based on their crystallographic parameters to the francolite composition of the coccoid structures and the coprolite groundmass. Overlapping peaks indicating a second generation of apatite on the XRD spectra were not observed. The EMP analyses in the micro-area, however, showed the occurrence of three different populations of apatite forming the bone fragments scattered within the coprolite groundmass. The first type of apatite occurs in the central part of the bone fragment (ESM Fig. 1A) and is characterized by higher content of SO_2 in the structure, ranging between 2.5 – 3.0 wt. %. The second type of apatite occurs in marginal part of the bones (ESM Fig. 1A) and contains stable quantity of SO_2 (2.25 – 2.5 wt. %). The phosphate content in marginal part is higher (32.6 – 33.8 P_2O_5 wt. %) than in the central part (ESM Fig. 1). The third type is represented by apatite

composing the bone fragments, but does not show any zonation in the BSE images (ESM Fig. 1B); its chemical composition is similar to the first type (ESM Fig. 1). However, these relatively small changes in chemical composition within the particular apatite generations do not need to significantly influence the structural parameters of the apatite types distinguished. The data may indicate that the chemical composition of bone apatite changed slowly during diagenesis. Depending on the rate and scale of the replacement of OH^- and phosphate ions by flourite and carbonate ions in the original bone structure (dahllite or hydroxylapatite), the fossil bone material preserves for a while the mosaic mineral composition with the simultaneous presence of two apatite phases (Nemliher et al., 2004). The described skeletal remains are formed only by francolite, which indicates a long time of diagenetic changes, started already during the Late Triassic period.

Figure 16 near here

4.4.2. Organic remains

In a number of samples (i.e., COP05, 08, 16), the organic residue was rich and differentiated in categories and taxa, while in other samples (i.e., COP02, 06, 09 and 18) the organic content was poor. In the remainder, only black and translucent organic particles were preserved, similar to plant or animal cuticles. The organic remains were grouped into six main groups: plant cuticles, plant tracheids, miospores (spores and pollen grains), animal cuticles, brown, translucent organic particles and black, opaque organic particles (Fig. 16). The identification of the recognizable cuticles revealed the presence of four cuticle types:

Cuticle type A (Fig. 17A-D). The cuticles are very robust and survived digestion and diagenesis almost completely. Epidermal cells are rectangular, occasionally polygonal, and isodiametric but elongate over veins. In most cases, epidermal cells are characterized by thick and straight anticlinal walls; the periclinal walls are smooth except for a central hollow papilla extending above the surface of the epidermis. Stomata are arranged in loose rows between veins. 4-

5 subsidiary cells encircle a deeply sunken stoma; each subsidiary cell bears a solid papilla that together cover the pit almost entirely. The ventral anticlinal walls of the subsidiary cells are strongly cutinized, as are the dorsal anticlinal walls occasionally, too. Subsidiaries are surrounded by one complete and occasionally another incomplete ring of additional subsidiary cells.

Cuticles of this type are almost identical with those published as *Lepidopteris ottonis* from the Rhaetian of Greenland (Harris, 1932), Scania (Lundblad, 1950) and Poland (Barbacka, 1991). Given the fact that these cuticles derived from coprolites and thus passed the digestive tract of the parent animal, a degradation of the cuticles and different preservation types are to be expected. Despite this, cuticles have apparently not been so heavily attacked by digestion as they looked rather “fresh” (cf. Harris, 1935; Lundblad, 1950).

Figure 17 near here

Cuticle type B (Fig. 17E-F). This cuticle is very delicate and anticlinal cell walls are almost invisible but the guard cells of the stomata have survived digestion and maceration quite properly. Epidermal cells are elongate over veins, but more polygonal in intercostal fields; anticlinal cell walls are straight and thin, producing distinct corners. Periclinal walls smooth, papillae absent. Stomata are regularly scattered between veins, orientated longitudinal, and flanked by large and strongly cutinized lateral subsidiary cells that create a sunken stomata. Polar cells are less strongly cutinized. Subsidiary cells have no papillae but strongly cutinized ventral and dorsal periclinal walls. The sunken guard cells apparently did not survive maceration.

This type of cuticle is very similar to different cuticles of *Podozamites* leaves, described from the Rhaetian of East Greenland (Harris, 1935). Of these, *Podozamites stewartensis* appeared as the most similar one. Certain identification could not be made because the preserved portions in the coprolites were too fragmentary.

Cuticle type C (Fig. 17G-I). This moderately delicate cuticle is characterized by elongate polygonal cells with acute short ends in many cases. Each cell is characterized by 3-5 roundish markings, which could either be papillae or other surface structures. However, the latter is not easy to depict. In one specimen, a stoma with two sunken, strongly cutinized guard cells is visible; further characteristics are, however, not to obtain. Due to the poor preservation of these cuticles, a further identification is almost impossible. The cuticles might be interpreted as bryophyte cuticles (cf. Reissinger, 1950; Hübers and Kerp, 2012), such as those reported by Harris (1931) from the Rhaetian of Jameson Land, Greenland.

Figure 18 near here

Cuticle type D (Fig. 18M). From one coprolite, a strongly "granulate" cuticle was obtained that has no signs of cells. The "granulae" could be interpreted as the densely spaced papillae of the small epidermal cells of the megaspore membrane or the cupulate disc of *Peltaspermum rotula* (cf. Harris, 1935; Lundblad, 1950; Barbacka, 1991). However, as no further details were visible, the identification remained ambiguous.

A considerable amount of woody elements found in the coprolites could be identified as tracheids with either bordered pits or with spirally or helically or even network-like arranged wall thickenings (Fig.18A-K). Most of these elements were quite intact but a further identification towards generic or specific level is impossible as no references are known to us from this time interval. Although rarely observed, some cuticles also show distinct signs of infestation by fungi (Fig. 18L).

4.4.3. Arthropod remains

Tiny arthropod remains are occasionally present in different coprolites (e.g., Northwood, 2005). Here, arthropods are represented by cuticle (Fig. 19) and a single ostracod valve (Fig. 13B).

The arthropod cuticles were very scarce in the investigated samples. Their highest frequency was close to 0.5-1% (COP01, 10 and 16), while in the rest of the samples (e.g. COP08), their frequency was much below 0.5% (Fig. 16). Their identification is hampered due to their small size, high degree of fragmentation and absence of preserved more diagnostic parts. However, the presence of a few distinct cuticle types (Fig. 19) point to the presence of different taxa. It is not excluded that they belonged to aquatic arthropods.

Figure 19 near here

A single ostracod valve was recognized in one specimen (Fig. 13B). The presence of ostracods in archosaur coprolites is common (Souoto, 2010), especially in crocodilian scats, probably because most of the archosaur coprolites were produced by animals living close to water environments or even in the shallow pools and swamps, usually full of small crustaceans. Recently, Khosla et al. (2015) reported numerous ostracods within putative titanosaurid coprolites from the Upper Cretaceous of India. Other small-sized aquatic crustaceans like conchostracans were also identified in coprolites from the Upper Permian of Russia (Owocki et al., 2012) and Early Triassic coprolites from Australia (Northwood, 2005).

5. Discussion

5.1. Molecular indicators

Molecular studies of Mesozoic vertebrate coprolites are rare. To our knowledge, the only detailed study on coprolite organic matter (OM) including OM pyrolysis was performed on two organic-poor coprolites from the Cretaceous Two Medicine Formation of NW Montana, USA (Hollacher et al., 2001). Biomarker data of Mesozoic coprolites have been presented on International Meeting of Organic Geochemistry in 1993 and described by Chin and Brassell

(1993). Lack of data from Palaeozoic to Mesozoic coprolites is probably due to the scarcity of well preserved, non-weathered material containing immature OM. More information comes from younger, excellently preserved Pleistocene to Holocene coprolites (e.g. van Geel et al., 2008; Gill et al., 2009; 2010; Carr et al., 2010), providing data about the nutritional habits and digestive processes of ancient animals.

The analysed Upper Triassic coprolite samples are unique due to very low thermal maturation of the rock sequence (not exceeding 0.35% of vitrinite reflectance; Marynowski et al., 2014) and their good preservation in green clay complex, without signs of weathering.

n-Alkane distribution with short chain homologues predomination is characteristic for bacterial organic matter type (Peters et al., 2005). However, dominance of odd-over-even homologues was observed in less abundant high molecular weight *n*-alkanes (Fig. 11), which is typical for terrestrial OM input. Series of mid-chain methyl-alkanes and cycloalkanes are most probably genetically connected with bacteria activity.

Distribution of short chain *n*-alkanoic acids and *n*-alkanols with even-carbon homologues predomination is characteristic for OM derived from bacteria (e.g. Hollocher et al., 2001), while even/odd dominance for long chain homologues suggests input from higher plants (e.g. Van Geelt et al., 2008). Distinctive dominance of $C_{16:0}$ and $C_{18:0}$ as well as high abundances of $C_{16:1}$ and $C_{18:1}$ FAs and alcohols can be genetically connected with bacteria and cyanobacteria (Fulco, 1983; Heath et al., 2002; Summons et al., 2013), but other sources, like higher animals and fishes (e.g. Thiel et al., 2014), or cutin from land plants (e.g. Hedges et al., 1997; Otto and Simoneit, 2001; Marynowski et al., 2007), cannot be definitely ruled out. In addition, two isoprenoidal FAs: 3,7,11,15-tetramethylhexadecanoic acid (phytanic acid) and 2,6,10,14-tetramethylpentadecanoic acid (pristanic acid) were also detected in low abundance (Table 5). They are most possibly degradation products of chlorophyll (e.g. Rontani and Volkmann, 2003), but what is noteworthy, both these compounds are constituents of marine and fresh-water fish oils (Corr et al., 2008).

Surprisingly, despite their old age, the coprolites contain sterols. Sitosterol is the major steroid compound in all samples, but cholesterol is also present in considerable amount. Two other sterols (campesterol and stigmasterol) are of low significance (Table 5). Coprostanol and other stanols, formed as biohydrogenation products of sterols in the gut of most higher animals and birds, and considered as biomarkers of faecal material (e.g. Sistiaga et al., 2014) were not found in the analysed samples. However, gut formation of stanols is typical mainly for mammals and even in this case varies a lot in intensity. For instance, the cholesterol-to-coprostanol conversion in human intestine can be almost complete or totally absent (Veiga et al., 2005). Moreover, the composition of faeces from herbivorous animals is more diverse than feces from carnivores and contains a much wider range of lipids (Gill and Bull, 2012). Sterols and steradienones distribution detected in Upper Triassic samples suggests diverse, plant-animal diet of the coprolite producers. Domination of sitosterol derived from higher plants over cholesterol genetically connected with higher animals does not necessarily mean that higher plants dominate in animal diet. It is well know that the decay rate of terrestrial OM is slower than for any other OM type and that land-derived material is, therefore, preferentially preserved in sediments (e.g. Prahl et al., 1997).

Glyceryl esters (palmitin and stearin isomers) are identified for the first time in coprolite samples (Table 5; Fig. 12). These compounds can be constituents of both plant and animal fats (e.g. Hilditch and Shrivastava, 1948; Shimi et al., 1959; Bosque-Sendra et al., 2012), and seem to be primary constituents of coprolite OM.

In all samples, a relatively low amount of urine was detected (Table 5). This finding suggests very fast mineralization of coprolites by apatite and preservation of OM from future decay/oxidation. Also occurrence of levoglucosan, an anhydrosugar formed by biomass burning, suggests very fast mineralization, especially since this compound is unstable and undergoes degradation in soils in thousands of years (Elias et al., 2001). The appearance of levoglucosan in coprolites is consistent with evidences of widespread wildfires detected in the Late Triassic bone-bearing clays (Marynowski and Simoneit, 2009; Marynowski et al., 2014). The other explanation of

the presence of such compounds in investigated samples is contamination by rainwaters with dissolved urine and levoglucosan. However, it seems unlikely that all coprolite samples were contaminated by these compounds.

5.2. Coccoid structures

The origin of the abundant, micrometre-sized, coccoid structures observed in the coprolites is under current debate. In the last decades, many studies have proposed a microbial origin for such cocci-like objects (e.g., Lamboy et al., 1994; Soudry, 1992; Cosmidis et al., 2013). Recently, it was shown experimentally that calcification induced by microorganisms could fossilize very delicate cell structures, including organic molecules and help preserving these structures against aging at relatively high temperature (Li et al., 2014). However, several authors have questioned the biogenicity of such biomorphic particles (e.g. Baturin and Titov, 2006) and it has been shown that hollow apatite spheres can be produced by abiotic processes (e.g., Gan et al., 2010; Perez et al., 2011). Recently, Cosmidis et al. (2013) interpreted similar coccoid structures in Eocene coprolites from the Ouled Abdoun phosphorites (Morocco), as Gram-negative bacteria fossilized by francolite. This was based on several lines of evidence: (1) The coccoid structures had a wall appearing as a dense francolite layer measuring between 20 and 40 nm in thickness, which corresponds to the thickness of a mineralized periplasm in Gram-negative bacteria (Benzerara et al., 2004). (2) Organic-richer layers were observed around the periplasm and were interpreted as fossil membranes similar to what was previously observed in experimental fossils (Miot et al., 2011). (3) Finally, they noted that the high density of coccoid structures in the Ouled Abdoun coprolites (~10^9 per cm^3) was similar to typical bacterial cell densities in modern reptilian scats.

The coccoid structures observed here in Late Triassic coprolites have a similar size, show a dense francolite wall and are sometimes filled or empty similarly to the coccoid structures in the Ouled Abdoun coprolites. In contrast, their walls seem a little thicker than periplasms and organic-

rich layers were not observed as in Ouled Abdoun coprolites. The coarser size of francolite crystals in Late Triassic coprolites is consistent with the older age of the sample and a possible higher degree of aging. Therefore, the differences between Late Triassic and Ouled Abdoun Eocene coccoid structures (disruption/disappearance of organic-rich layers and thicker wall) could be due to a more advanced aging and/or different early taphonomic processes. In any case, the high density of these structures in coprolites which originally contained a high density of coccoid Gram-negative bacteria holds as a strong support for an interpretation of such structures as phosphatized bacteria. Other types than just Gram-negative bacteria may have fossilized but more specific characterization of the identity of the fossils is difficult to obtain at that scale (Cosmidis et al., 2013).

Another, independent support for the bacterial nature of the preserved coccoid structures is provided by the presence of specific biomarkers, like mid-chain methyl-alkanes and cycloalkanes, or short chain *n*-alkanoic acids and *n*-alkanols with even-carbon homologues predomination, as well as distinct dominance of $C_{16:0}$ and $C_{18:0}$ and high abundances of $C_{16:1}$ and $C_{18:1}$ FAs and alcohols.

5.3. Coprolite producers

Deciphering which animal is responsible for coprolite production is always speculative, as by the definition they are preserved outside the producer's body (e.g., Thulborn, 1991; Hunt et al., 1994; Chin, 2002; Bajdek et al., 2014). Thus, the animal remains associated with coprolites in the same deposits are very often used as an indication of potential coprolite producers. Association of coprolites with only one or two kinds of animal groups offers an easier task. In contrast, assemblages consisting of several different vertebrate groups may pose a serious problem for interpreting potential animal responsible for defecation of digested remains. Sometimes, the morphology of the coprolites does not allow for their easy linking with associated animal, leading to the conclusions that coprolites may have been produced by yet undiscovered animals (e.g., Jain, 1983). In other cases, the characteristic features of coprolites, e.g., exceptionally large size (e.g.,

Chin et al., 1998, for tyrannosaurid coprolites) or characteristic composition and association (e.g., Fiorelli et al., 2013, for dicynodont coprolites), may very intuitively point to the exact producer.

From the size, morphology, and phosphatic composition of the specimens, it can be inferred that all coprolites described here were produced by carnivores (e.g., Chin, 2002). However, taking the coprolite size into account when interpreting the size of a potential producer may be very problematic. For example, the Upper Triassic coprolites from Argentina studied by Hollocher et al. (2005) were interpreted as produced by an animal having 5-15 kg, as based on the coprolite diameter (20 and 21 mm). This may equally indicate that the coprolites may have been produced by a single species on various growth stages, or by a variety of species having different sizes. Also the shape of the coprolites is not helpful either, since a high intraspecific variation in morphology has been shown. For example, distinguishing scats of modern crocodilian species is impossible (Milàn, 2012).

Some of the studied coprolites representing morphotype 1 (COP02, 04a and 06) and morphotype 2 (COP01 and 14) contain only bone material (plant remains are very scarce, see Fig. 15) suggesting that the producers were strictly carnivorous. Some small-sized specimens (COP01) could have originated from some small to medium-sized archosaurs or temnospondyl amphibians, like *Cyclotosaurus* sp. or *Gerrothorax* sp. known from the deposits sampled. The larger, elongated coprolites (COP04a, 06, 14) may have been produced by a medium to large-sized archosaurs. When compared with the recent crocodilian scats (Milàn, 2012) or undisputed predatory dinosaur coprolites from Jurassic or Cretaceous, the resemblance is strong (e.g., Chin et al., 1998; Chin, 2002). In addition, comparative studies show that modern animals with a carnivorous diet such as crocodilians or big cats tend to produce faecal masses with a cylindrical structure (Stuart and Stuart, 1998; Chame, 2003; Souto, 2010; Milàn, 2012). The studied coprolites are associated with bone-bearing clays. The fossil carnivore archosaur fauna of the Poręba site (Fig. 3) is composed of large, but still undescribed, predatory archosaur (probably similar to *Smok wawelski* from Lisowice), herrerasaurid, theropod, and possibly neotheropod (Sulej et al., 2012; Niedźwiedzki et al., 2014).

Palaeochersis-like turtles are also known from the Poręba site (Sulej et al., 2012) but rather this can be excluded from a group of possible coprolite producers. The carnivore fauna from Lisowice site (Fig. 5) contains small-sized poposaurid archosaur, small-sized predatory dinosaur and dinosauriform, and the large early predatory dinosaur *Smok wawelski* (Niedźwiedzki et al., 2012; Niedźwiedzki, 2015). Thus, the described coprolites fall inside the size-range of medium to large archosaurs from the mentioned faunistic elements. Fossils of large temnospondyls (*Cyclotosaurus* sp.) also occur in both sites. We cannot exclude that capitosauroids also produced the large and medium-sized coprolites from Poręba and Lisowice, especially since some coprolites contain fish scales, perhaps suggesting for at least a periodical aquatic life-style of some of the producers.

One characteristic feature of elongated (morphotype 1) or irregularly shaped (morphotype 3) coprolites is the presence of not only bone fragments inside, but also abundant plant remains in the form of cuticles, tracheids/wood remains, megaspores and pollen grains, as well as closely unrecognizable black and brown organic particles. Recently, phosphatic coprolites containing plant debris have also been described from the Late Cretaceous of India by Khosla et al. (2015). As coprolites putatively produced by herbivores contain only plant inclusions and lack phosphate mineralization (e.g., Chin and Kirkland, 1998; Chin, 2007; Fiorelli et al., 2013; Bajdek et al., 2014), the presence of various plant debris preserved within the phosphatic coprolites, which are usually characteristic for carnivores, is interesting and worth of discussion. Moreover, plant remains not only occur in small-sized (20 mm in diameter) coprolites, but also in the largest specimens (30–50 mm in diameter) investigated here. Their accidental occurrence in the coprolites, e.g., due to adhesion to deposited faeces, is unlikely as all were derived from inside the coprolites. The good preservation of woody elements and cuticles would suggest that the animals were feeding on living plants, mainly foliage but also swallowed some wood, and were not able to degrade down lignin and cutin/cutan, both of which are complex polymers usually degraded by specialized fungi. In only one instance, the cuticle bears a distinct sign of fungal infestation (Fig. 18L) but it is unclear

whether it happened before the plant was swallowed by the animal, or after the remains were defecated.

The association of animal and plant remains in the phosphatic coprolites suggests that potential coprolite producers were 1) omnivorous, feeding on both animals and plants, or 2) carnivorous, ingesting occasionally plants, or 3) strictly carnivorous, swallowing accidentally plant material during feeding. The majority of terrestrial vertebrates from investigated sites consist of carnivores, mainly archosaurs. Indeed, a tooth of a predatory archosaur found in one of the coprolites (Niedźwiedzki, 2015) strongly attests for the carnivore nature of some of the producers. The only candidates, which could feed on both animals and incidentally (or accidentally) plants were temnospondyls, turtles, poposaurids and other aquatic archosaurs. Temnospondyls, spending much time in an aquatic habitat, could have incidentally, as well as accidentally, swallowed plant remains when hunting on animal preys. Turtles more likely could have swallowed both animal (fish) prey and plant remains (e.g., Northwood, 2005). The poposaurids from Lisowice, when hunting close to the aquatic environment, could also have accidentally swallowed some plant fragments. The presence of an ostracod and arthropod cuticles (some of which could belonged to aquatic species) in some of the coprolites may suggest such a possibility (e.g., Northwood, 2005). It is known that during feeding, wild alligators sometimes swallow plant material (see Keenan et al., 2013). Finally, it is highly possible that some coprolite producers were strictly carnivorous and plant material might have been swallowed together with other animals in the form of the gastrointestinal content of the latter (e.g., Thulborn, 1991). This may be supported by the presence of a single type of cuticle in some of the coprolites (e.g., *Lepidopteris* in coprolites COP05, 08-10 and *Podozamites* in coprolites COP06-07 and 16), suggesting that prey animals would preferentially feed on specific plants growing in the area. Predation on herbivorous animals are also documented by the presence of dicynodont bone fragments in two coprolites studied by Niedźwiedzki (2015), as well as the presence of dicynodont bones with preserved bite-marks (Niedźwiedzki et al., 2011). Recently, putative dicynodont coprolites full of plant debris have also been documented from the

Lisowice site (Bajdek et al., 2014). Thus, such accidental swallowing of plant remains by strictly carnivorous vertebrates during predation or scavenging may have occurred. As shown above, the mixed animal-plant remains are well-expressed in the biomarker composition of the studied coprolites. However, the phytanic and pristanic acids, which are possible degradation products of chlorophyll, also occur in fish oils. If so, it may be additional geochemical evidence that the diet of at least some of the coprolite producers relied on fish. Thus, their foraging in or near the aquatic habitat could have resulted in accidental swallowing of plant material as well. In that case, some semi-aquatic archosaurs and/or temnospondyls could have been probable culprits.

Vertebrate inclusions (scales, teeth and bones) can be well-preserved or show breakage and some degree of digestion by stomach acids (Fig. 13C, 15B, F). Some components also show degradation by microbes (Fig. 13F, 15C-E), which most probably attacked the bony material for organic residues when they were already defecated. The survival of bony material suggests that the coprolite producers did not digest bones completely as extant crocodilians do (e.g., Milàn, 2012). It suggests that such total bone digestion were not universal among archosauromorphs in the past (Chin et al., 1998).

6. Conclusions

Vertebrate coprolites derived from the Upper Triassic terrestrial bone-bearing deposits have been investigated using various analytical methods in order to decipher their composition, potential producers' diet and nature of the preserved microbial structures. The coprolite groundmass is composed of carbonate-rich fluorapatite (francolite) preserving abundant, micrometre-sized coccoid structures interpreted as fossilized bacteria, which may have mediated the phosphatization of the original faeces. The bacterial nature of the preserved coccoid structures may be supported by specific biomarkers, such as *n*-alkanes with predomination of short chain homologues and

dominance of $C_{16:0}$ and $C_{18:0}$ fatty acids and alcohols as well as high abundances of $C_{16:1}$ and $C_{18:1}$ fatty acids.

The coprolites include specimens, which exclusively contain vertebrate material and those, which contain both vertebrate fragments and plant remains. The vertebrate material, in the form of bones, scales and teeth fragments are preserved in different conditions, ranging from well-preserved to remains at different stages of digestion. Those coprolites with only vertebrate remains are suggestive for exclusive carnivorous diet of the producers. The interpretation of coprolites consisting of both vertebrate and plant remains is more debatable. Although the producers of such coprolites may have been omnivorous animals, it is highly probable that they were carnivorous which only occasionally ingested plants, or swallowed them accidentally during predation or scavenging upon other herbivorous animals which previously fed on plants.

The probable culprits swallowing animal prey and occasionally plants may have been animals that foraged in or near aquatic habitats, such as some semi-aquatic archosaurs and/or temnospondyls. This may be partly supported by the presence of such specific biomarkers as phytanic and pristanic acids, which are constituents of fish oil. The coprolites were mineralized on very early stages of diagenesis and were not affected by late/extensive diagenesis, which is supported by the preservation of labile organic compounds, such as sterols, palmitin, stearin or levoglucosan.

The multidisciplinary approach performed in the study of these coprolites provides valuable data on diverse specific problems. Yet the question about the identity of the producer remains challenging, especially when the coprolites were associated together with remains belonging to a variety of vertebrate species as in the present case.

Acknowledgments

The authors thank Bernd R.T. Simoneit (Oregon) for help in identification of some polar compounds. This project was primarily financed by MNiSW grant N N307 066040 (to MZ) and partly by the project No. 3941/B/P01/2009/36 (to GN). GN is currently funded by grant awarded to Per Erik Ahlberg (Uppsala University).

References

Aldridge, R.J., Gabbott, S.E., Siveter, L.J., Theron, J.N., 2006. Bromalites from the Soom Shale lagerstatte (Upper Ordovician) of South Africa: Palaeoecological and palaeobiological implications. Palaeontology 49, 857–871.

Bajdek, P., Owocki, K., Niedźwiedzki, G., 2014. Putative dicynodont coprolites from the Upper Triassic of Poland. Palaeogeography, Palaeoclimatology, Palaeoecology 411, 1–17.

Barbacka, M., 1991. *Lepidopteris ottonis* (Goepp.) Schimp. and *Peltaspermum rotula* (Harris) from the Rhaetian of Poland. Acta Palaeobotanica 31, 23–47

Bastow, T.P., van Aarssen, B.G.K., Lang, D., 2007. Rapid small-scale separation of saturate, aromatic and polar components in petroleum. Organic Geochemistry 38, 1235–1250.

Baturin, G.N., Titov, A.T., 2006. Biomorphic formations in recent phosphorites. Oceanology 46, 711–715

Benzerara, K., Menguy, N., Guyot, F., Skouri, F., de Lucca, G., Heulin, T., 2004. Bacteria-controlled precipitation of calcium phosphate by *R. tataouinensis*. Earth and Planetary Science Letters 228, 439–449.

Benzerara, K., Yoon, T.H., Menguy, N., Tyliszczak, T., Brown, G., 2005. Nanoscale environments associated with bioweathering of a meteoritic Mg-Fe-Pyroxene. Proceedings of the National Academy of Sciences 102, 979–982.

Bernard, S., Benzerara, K., Beyssac, O., Brown Jr., G.E., 2010. Multiscale characterization of pyritized plant tissues in blueschist facies metamorphic rocks. Geochimica et Cosmochimica Acta 74, 5054–5068.

Bluhm, H., Andersson, K., Araki, T., Benzerara, K., Brown, G.E., Dynes, J.J., Ghosal, S., Gilles, M.K., Hansen, H.C., Hemminger, J.C., Hitchcock, A.P., Ketteler, G., Kilcoyne, A.L.D., Kneedler, E., Lawrence, J.R., Leppard, G.G., Majzlan, J., Mun, B.S., Myneni, S.C.B., Nilsson, A., Ogasawara, H., Ogletree, D.F., Pecher, K., Salmeron, M., Shuh, D.K., Tonner, B., Tyliszczak, T., Warwick, T., Yoon, T.H., 2006. Soft X-ray microscopy and spectroscopy at the molecular environmental science beamline at the Advanced Light Source. Journal of Electronic Spectroscopy and Related Phenomena 150, 86–104.

Bosque-Sendra, J.M, Cuadros-Rodríguez, L., Ruiz-Samblás, C., de la Mata, A.P., 2012. Combining chromatography and chemometrics for the characterization and authentication of fats and oils from triacylglycerol compositional data-a review. Analytica Chimica Acta 724, 1–11.

Brusatte, S.L., Nesbitt, S.J., Irmis, R.B., Butler, R.J., Benton, M.J., Norell, M.A., 2010. The origin and radiation of dinosaurs. Earth-Science Reviews 101, 68–100.

Budziszewska-Karwowska, E., Bujok, A., Sadlok, G., 2010. Bite marks on an Upper Triassic dicynodontid tibia from Zawiercie, Kraków-Częstochowa Upland, southern Poland. Palaios 25, 415–421.

Carlut, J., Benzerara, K., Horen, H., Menguy, N., Janots, D., Findling, N., Addad, A., Machouk, I., 2010. Microscopy study of biologically mediated alteration of natural mid-oceanic ridge basalts and magnetic implications. Journal of Geophysical Research 115, G00G11,doi:10.1029/2009JG001139.

Carr, A.S., Boom, A., Chase, B.M., 2010. The potential of plant biomarker evidence derived from rock hyrax middens as an indicator of palaeoenvironmental change. Palaeogeography, Palaeoclimatology, Palaeoecology 285, 321–330.

Chame, M., 2003. Terrestrial mammal feces: a morphometric summary and description. Mem. Inst. Oswaldo Cruz 98 (Suppl. I), 71–94.

Chin, K., 2002. Analyses of coprolites produced by carnivorous vertebrates, In: Kowalewski, M., Kelley, P.H. (Eds), Predation in the Fossil Record, Palaeontological Society Papers 8, pp. 43–49.

Chin, K., 2007. The paleobiological implications of herbivorous dinosaur coprolites from the Upper Cretaceous Two Medicine Formation of Montana: why eat wood? Palaios 22, 554–566.

Chin, K., Brassell, S.C., 1993. The biomarker composition of coprolites from marine and terrestrial vertebrates: an untapped source of paleoecological information. In: Øygard, K., (Ed.), Organic Geochemistry Poster Sessions from the 16th International Meeting on Organic Geochemistry, Stavanger, 444–447.

Chin, K., Kirkland, J.I., 1998. Probable herbivore coprolites from the Upper Jurassic Mygatt-Moore Quarry, Western Colorado. Modern Geology 23, 249–275.

Chin, K., Tokaryk, T.T., Erickson, G.M., Calk, L.C., 1998. A king-sized theropod coprolite. Nature 393, 680–682.

Chin, K., Eberth, D.A., Schweitzer, M.H., Rando, T.A., Sloboda, W.J., Horner, J.R., 2003. Remarkable preservation of undigested muscle tissue within a Late Cretaceous tyrannosaurid coprolite from Alberta, Canada. Palaios 18, 286–294.

Chin, K., Hartman, J.H., Roth, B., 2009. Opportunistic exploitation of dinosaur dung: fossil snails in coprolites from the Upper Cretaceous Two Medicine Formation of Montana. Lethaia 42, 185–198.

Corr, L.T., Richards, M.P., Jim, S., Ambrose, S.H., Mackie, A., Beattie, O., Evershed, R.P., 2008. Probing dietary change of Kwäday Dän Ts'ìnchi, an ancient glacier body from British Columbia: I. Complementary use of marine lipid biomarker and carbon isotope signatures as novel indicators of a marine diet. Journal of Archaeological Science 35, 2102–2110.

Cosmidis, J., Benzerara, K., 2014. Soft X-ray scanning transmission spectro-microscopy. In: DiMasi, E., Gower, L.B. (Eds.), Biomineralization Sourcebook: Characterization of Biominerals and Biomimetic Materials. CRC Press.

Cosmidis, J., Benzerara, K., Nassif, N., Tyliszczak, T., Bourdelle, F., 2014. Characterization of Ca-phosphate biomaterials by scanning transmission X-ray microscopy (STXM) at the Ca $L_{2,3}$-, P $L_{2,3}$- and C K-edges. Acta Biomaterialia, doi:10.1016/j.actbio.2014.10.003.

Cosmidis, J. Benzerara, K. Gheerbrant, E, Esteve, I., Bouya, B., Amaghzaz, M. 2013. Nanometer-scale characterization of exceptionally preserved bacterial fossils in Paleocene phosphorites from Ouled Abdoun (Morocco). Geobiology 11, 139–153.

Dentzien-Dias, P.C., Poinar, G., Jr., de Figuereido, A.E., Pacheco, A.C., Horn, B.L., Schultz, C.L., 2013. Tapeworm eggs in a 270 million-year-old shark coprolite. PLoS ONE 8(1):e55007. doi: 10.1371/journal.pone.0055007.

Dzik, J., Sulej, T., 2007. A review of the early Late Triassic Krasiejów biota from Silesia, Poland. Palaeontologia Polonica, 64, 3–27.

Dzik, J., Sulej, T., Niedźwiedzki, G., 2008. A dicynodont-theropod association in the latest Triassic of Poland. Acta Palaeontologica Polonica 53, 733–738.

Edwards, D., Selden, P.A., Axe, L., 2012. Selective feeding in an Early Devonian terrestrial ecosystem. Palaios 27, 509–522.

Elias, V.O., Simoneit, B.R.T., Cordeiro, R.C., Turcq, B. 2001. Evaluating levoglucosan as an indicator of biomass burning in Carajas, Amazonia: A comparison to the charcoal record. Geochimica et Cosmochimica Acta, 65, 267–272.

Eriksson, M.E., Lindgren, J., Chin, K., Mansby, U., 2011. Coprolite morphotypes from the Upper Cretaceous of Sweden: novel views on an ancient ecosystem and implications for coprolite taphonomy. Lethaia 44, 455–468.

Fiorelli, L.E., Ezcurra, M.D., Hechenleitner, E.M., Argañaraz, E., Taborda, J.R.A., Trotteyn,M.J., Belén von Baczko, M., Desojo, J.B., 2013. The oldest known communal latrines provide

evidence of gregarism in Triassic megaherbivores. Scientific Reports 3, 3348. http://dx.doi.org/10.1038/srep03348.

Franz, M., Bachmann, G.H., Beutler, G., 2007a. Retyk sensu polonico versus Rhaet sensu germanico—new results. Schriftenreihe der Deutschen Gesellschaft für Geowissenschaften 53: 99–100.

Franz, M., Bachmann, G.H., Beutler, G., 2007b. Sedimentology and Facies of the Polish Retyk and the German Arnstadt and Exter Formations (Norian, Rhaetian) in the eastern Central European Basin (CEB). Schriftenreihe der Deutschen Gesellschaft für Geowissenschaften 53, 101.

Franz, M., 2008. Litho- und Leitflächenstratigraphie, Chronostratigraphie, Zyklo- und Sequenzstratigraphie des Keupers im östlichen Zentraleuropäischen Becken (Deutschland, Polen) und Dänischen Becken (Dänemark, Schweden). PhD Thesis. Martin-Luther-Universität HalleWittenberg, 197 pp.

Fulco, A.J., 1983. Fatty acid metabolism in bacteria. Progress in Lipid Research 22, 132–160.

Gan, Y., Han, D., Gu, F., Wang, Z., Guo, G., 2010. Biomimetic synthesis of calcium-strontium apatite hollow nanospheres. Science China Chemistry 53, 1723–1727.

Gill, F.L., Bull, I.D., 2012. Lipid analysis of vertebrate coprolites: New Mexico Museum of Natural History and Science, Bulletin 57, 93–98.

Gill, F.L., Crump, M.P., Schouten, R., Bull, I.D., 2009. Lipid analysis of a ground sloth coprolite, Quaternary Research 72, 284–288.

Gill, F.L., Dewhurst, R.J., Dungait, J.A.J., Evershed, R.P., Ives, L., Li, C.S., Pancost, R.D., Sullivan, M., Bera, S., Bull, I.D., 2010. Archaeol - a biomarker for foregut fermentation in modern and ancient herbivorous mammals? Organic Geochemistry 41, 467–472.

Golonka, J., 2007. Late Triassic and Early Jurassic paleogeography of the world. Palaeogeography, Palaeoclimatology, Palaeoecology 244, 297–307.

Harris, T.M., 1926. The Rhaetic flora of Scoresby Sound East Greenland. Meddelelser om Grønland 68, 43–148.

Harris, T.M., 1931. The fossil flora of Scoresby Sound East Greenland. Part 1: Cryptogams (exclusive of Lycopodiales). Meddelelser om Grønland, 85, 1–104.

Harris, T.M., 1932. The fossil flora of Scoresby Sound East Greenland.Part 2: description of seed plants incertae sedis together with a discussion of certain cycadophyte cuticles. Meddelelser om Grønland 85, 1–112.

Harris, T.M., 1935. The fossil Flora of Scoresby Sound East Greenland. Part 4. Ginkgoales, Coniferales, Lycopodiales and isolated fructifications. Meddelelser om Grønland 112, 1–176.

Heath, R.J., Jackowski, S., Rock, Ch.O., 2002. Fatty acid and phospholipid metabolism in prokaryotes. In: D.E. Vance, Vance, J.E., (Eds.), Biochemistry of lipids, lipoproteins and membranes (4th Edn.), Elsevier, 55–92.

Hedges, J.I., Keil, R.G., Benner, R., 1997. What happens to terrestrial organic matter in the ocean? Organic Geochemistry 27, 195–212.

Heunisch, C., 1999. Die Bedeutung der Palynologie fur Biostratigraphie und Fazies in der Germanischen Trias. 207–220. In: Hauschke, N., Wilde, V., (Eds.), Trias, Eine ganz andere Welt, Mitteleuropa im fruhen Erdmittelalter. Verlag Dr Friedrich Pfeil, Munchen, 647 pp.

Hilditch, T.P., Shrivastava, R.K., 1948. The component fatty acids of a yeast fat. Biochimica et Biophysica Acta 2, 80–85.

Hollocher, T.C., Chin, K., Hollocher, K.T., Kruge, M.A., 2001. Bacterial residues in coprolite of herbivorous dinosaurs: role of bacteria in mineralization of feces. Palaios 16, 547-565.

Hollocher, K.T., Alcober, O.A., Colombi, C.E., Hollocher, T.C., 2005. Carnivore coprolites from the Upper Triassic Ischigualasto Formation, Argentina: chemistry, mineralogy, and evidence for rapid initial mineralization. Palaios 20, 51–63.

Hollocher, K.T., Hollocher, T.C., Rigby, Jr., J.K., 2010. A phosphatic coprolite lacking diagenetic permineralization from the Upper Cretaceous Hell Creek Formation, Northeastern Montana: Importance of dietary calcium phosphate in presevation. Palaios 25, 132–140.

Hübers, M., Kerp, H., 2014. Oldest known mosses discovered in Mississippian (late Visean) strata of Germany. Geology 40, 755–758.

Hunt, A.P., Lucas, S.G., 2005a. A new coprolite ichnotaxon from the Early Permian of Texas. In: Lucas, S.G., Zeigler, K.E. (Eds.), The Nonmarine Permian. New Mexico Museum of Natural History and Science Bulletin 30, 121–122.

Hunt, A.P., Lucas, S.G., 2005b. The origin of large vertebrate coprolites from the Early Permian of Texas. In: Lucas, S.G., Zeigler, K.E. (Eds.), The Nonmarine Permian. New Mexico Museum of Natural History and Science Bulletin 30, 125–126.

Hunt, A.P., Lucas, S.G., Spielmann, J.A., Lerner, A.J., 2007. A review of vertebrate coprolitesof the Triassic with descriptions of new Mesozoic ichnotaxa, In: Lucas, SG., Spielmann, J.A. (Eds.), The Global Triassic. New Mexico Museum of Natural History and Science Bulletin 41, 88–107.

Hunt, A.P., Lucas, S.G., Lockley, M.G., 1998. Taxonomy and stratigraphic and facies significance of vertebrate coprolites of the Upper Triassic Chinle Group, Western United States. Ichnos 5, 225–234.

Hunt, A.P., Chin, K., Lockley, M.G., 1994. The paleobiology of vertebrate coprolites. In: Donovan, S.K. (Ed.), The Paleobiology of Trace Fossils. John Wiley, London, pp. 221–240.

Jain, S.L., 1983. Spirally coiled “coprolites” from the Upper Triassic Maleri Formation, India. Palaeontology 26, 813–829.

Khosla, A., Chin, K., Alimohammadin, H., Dutta, D., 2015. Ostracods, plant tissues, and other inclusions in coprolites from the Late Cretaceous Lameta Formation at Pisdura, India: Taphonomical and palaeoecological implications. Palaeogeography, Palaeoclimatology, Palaeoecology 418, 90–100.

Kubik, R., Uhl, D., Marynowski, L., 2014. Evidence of wildfires during deposition of the Upper Silesian Keuper succession. Annales Societatis Geologorum Poloniae, 84 (in press).

Kurschner, W.M., Herngreen, G.F., W. 2010. Triassic palynology of central and northwestern Europe: a review of palynofloral diversity patterns and biostratigraphic subdivisions.. In Lucas, S.G., (Ed.), The Triassic timescale. Geological Society, London, Special Publication 334, 263–283.

Lamboy, M., Rao, V.P., Ahmed, E., Azzouzi, N., 1994. Nannostructure and significance of fish coprolites in phosphorites. Marine Geology 120, 373–383.

Larsson, L.M., 2003. Late Triassic and Early Jurassic palynology of the Höganäs Basin and the Ängelholm Trough, NW Scania, Sweden. Master thesis, Lund University No. 158, 20 pp.

Li, J., Bernard, S., Benzerara, K., Allard, T., Cosmidis, J., Moussou, J., Beyssac, O., 2014. Impact of biomineralization on the preservation of microorganisms during fossilization: an experimental perspective. Earth and Planetary Science Letters 400, 113–122.

Lund, J.J., 1977. Rhaetic to Lower Liassic palynology of the onshore south-eastern North Sea Basin. Danmarks Geologiska Undersøgelse 2, 1–105.

Lundblad, A.B., 1950. Studies in the Rhaeto–Liassic floras of Sweden. I. Pteridophyta, Pteridospermae and Cycadophyta from the mining district of NW Scania. Kungliga Svenska Vetenskapsakademiens Handlingar, Fjärde Serien 1, 1–82.

Ma, Y., Chen, C.T., Meigs, G., Randall, K., Sette, F., 1991. High resolution K-shell photoabsorption measurements of simple molecules. Physical Review A 44, 1848–1858.

Mahaney, W,C., Barendregt, R.W., Allen, C.C.R., Milner, M.W., Bray, D., 2013. Coprolites from the Cretaceous Bearpaw Formation of Saskatchewan. Cretaceous Research 41, 31–38.

Mancuso, A.C., Marsicano, C., Palma, R., 2004. Vertebrate coprolites from the Triassic of Argentina. Ameghiniana 41, 347–354.

Marynowski L., Wyszomirski P., 2008. Organic geochemical evidences of early diagenetic oxidation of the terrestrial organic matter during the Triassic arid and semiarid climatic conditions. Applied Geochemistry 23, 2612–2618.

Marynowski, L., Zatoń, M., Simoneit, B.R.T., Otto, A., Jędrysik, M.O., Grelowski, C., Kurkiewicz S., 2007. Compositions, sources and depositional environments of organic matter from the Middle Jurassic clays of Poland. Applied Geochemistry 22, 2456–2485.

Marynowski, L., Kubik, R., Uhl, D., Simoneit, B.R.T., 2014. Molecular composition of fossil charcoal and relationship with incomplete combustion of wood. Organic Geochemistry 77, 22–31.

Meng, J., Wyss, A.R., 1997. Multituberculate and other mammal hair recovered from Palaeogene excreta. Nature 385, 712–714.

Milàn, J., 2012. Crocodylian scatology - a look into morphology, internal architecture, inter- and intraspecific variation and prey remains in extant crocodylian feces. New Mexico Museum of Natural History and Science bulletin 57: 65-71.

Miot J., MacLellan, K., Boisset, N., Benzerara, K., 2011. Preservation of protein globules and peptidoglycan in the mineralized cell wall of nitrate-reducing iron(II) oxidizing bacteria: a cryo-electron microscopy study. Geobiology 9, 459–470.

Nakajima, Y., Izumi, K., 2014. Coprolites from the upper Osawa Formation (upper Spathian), northeastern Japan: Evidence for predation in a marine ecosystem 5 Myr after the end-Permian mass extinction. Palaeogeography, Palaeoclimatology, Palaeoecology 414, 225–232.

Nemliher, J.G., Baturin, G.N., Kallaste, T.E., Murdmaa, I.O., 2004. Transformation of hydroxyapatite of bone phosphate from the ocean bottom during fossilization. Lithology and Mineral Resources 39, 468–479.

Niedźwiedzki, G., 2015 (in press). The large predatory archosaur *Smok wawelski* from the latest Triassic of Poland. Palaeontologia Polonica 67.

Niedźwiedzki, G., Sulej, T., Dzik, J., 2012. A large predatory archosaur from the Late Triassic of Poland: Acta Palaeontologica Polonica 57, 267–276.

Niedźwiedzki, G., Brusatte, S.L., Sulej, T., Butler, R.J., 2014. Basal dinosauriform and theropod dinosaurs from the mid–late Norian (Late Triassic) of Poland. Implications for Triassic dinosaur evolution and distribution. Palaeontology 57, 1121–1142.

Northwood, C., 2005. Early Triassic coprolites from Australia and their palaeobiological significance. Palaeontology 48, 49–68.

Ociepa, A.-M., Staneczko, K., Feldman-Olszewska, A., Barbacka, M., 2008. Nowe stanowiska *Lepidopteris ottonis* (Goeppert) Schimper w Polsce. In: Krobicki, M, (Ed.), Utwory przełomu jury i kredy w zachodnich Karpatach fliszowych polsko-czeskiego pogranicza, Jurassica VII. Geologia 34, 199–200.

Olsen, P.E., Kent, D.V., Sues, H.D., Koeberl, C., Huber, H., Montanari, A., Rainforth, E.C., Fowell, S.J., Szajna, M.J., Hartline, B.W., 2002. Ascent of dinosaurs linked to an iridium anomaly at the Triassic-Jurassic boundary. Science 296, 1305–1307.

Orłowska-Zwolińska, T., 1983. Palynostratigraphy of the upper part of Triassic epicontinental sediments in Poland. Prace Instytutu Geologicznego 104, 1–88.

Orłowska-Zwolińska, T., 1985, Palynological zones of the Polish epicontinental Triassic. Bulletin of the Polish Academy of Sciences–Earth Sciences 33, 107–117.

Otto, A., Simoneit, B.R.T., 2001. Chemosystematics and diagenesis of terpenoids in fossil conifer species and sediment from the Eocene Zeitz formation, Saxony, Germany. Geochimica et Cosmochimica Acta 65, 3505–3527.

Owocki, K., Niedźwiedzki, G., Sennikov, A.G., Golubev, V.K., Janiszewska, K., Sulej, T., 2012. Upper Permian vertebrate coprolites from the Vyazniki and Gorokhovets, Vyatkian regional stage, Russian Platform. Palaios 27, 867–877.

Pacyna, G., 2014. Plant remains from the Polish Triassic. Present knowledge and future prospects. Acta Palaeobotanica 54, 3–33.

Perez, R.A., Del Valle, S., Altankov, G., Ginebra, M.-P., 2011. Porous hydroxyapatite and gelatin/hydroxyapatite microspheres obtained by calcium phosphate cement emulsion. Journal of Biomedical Materials Research Part B: Applied Biomaterials 97B, 156–166.

Peters, K.E., Walters, C.C., Moldowan, J.M., 2005. The Biomarker Guide Volume 1. University Press, Cambridge, United Kingdom, 471 pp.

Pieńkowski, G., Niedźwiedzki, G., Brański, P., 2014. Climatic reversals related to the Central Atlantic magmatic province caused the end-Triassic biotic crisis— Evidence from continental strata in Poland. In: Keller, G., Kerr, A., (Eds.), Volcanism, Impacts, and Mass Extinctions: Causes and Effects. Geological Society of America Special Paper 505, 263-286.

Prahl, F.G., De Lange, G.J., Scholten, S., Cowie, G.L., 1997. A case of post-depositional aerobic degradation of terrestrial organic matter in turbidite deposits from the Madeira Abyssal Plain. Organic Geochemistry 34, 1–35.

Reissinger, A., 1950. Die “Pollenanalyse” ausgedehnt auf alle Sedimentgesteine der geologischen Vergangenheit: Zweiter Teil. Palaeontographica Abt B 40, 99–126.

Rontani, J-F., Volkman, J.K., 2003. Phytol degradation products as biogeochemical tracers in aquatic environments. Organic Geochemistry 27, 141–152.

Schoene, B., Guex, J., Bartolini, A., Schaltegger, U., Blackburn, T., 2010. Correlating the end-Triassic mass extinction and flood basalt volcanism at the 100 ka level. Geology 38, 387–390.

Shen, C., Pratt, B.R., Zhang, X.-g., 2014. Phosphatized coprolites from the middle Cambrian (Stage 5) Duyun fauna of China. Palaeogeography, Palaeoclimatology, Palaeoecology 410, 104–112.

Shimi, I. R., Singh, J., Walker, T. K., 1959. The component fatty acids of *Penicillium spinulosum* fat. Biochemical Journal 72, 184–187.

Sistiaga, A., Berna, F., Laursen, R., Goldberg, P., 2014. Steroidal biomarker analysis of a 14,000 years old putative human coprolite from Paisley Cave, Oregon. Journal of Archaeological Science 41, 813–817.

Smith, R.M.H., Botha-Brink, J., 2011. Morphology and composition of bone-bearing coprolites from the Late Permian Beaufort Group, Karoo Basin, South Africa. Palaeogeography, Palaeoclimatology, Palaeoecology 312, 40–53.

Soudry, D., 1992. Primary bedded phosphorites in the Campanian Mishash Formation, Negev, Southern Israel. Sedimentary Geology 80, 77–88.

Souto, P.R.F., 2010. The crocodylomorph coprolites from Barum Basin, Upper Cretaceous, Brazil: New Mexico Museum of Natural History and Science, Bulletin 51, 201–208.

Staneczko, K., 2007. Nowe dane paleobotaniczne na temat górnego triasu z Lipia Śląskiego koło Lublińca (południowa Polska). Geo-Sympozjum Młodych Badaczy Silesia 2007, 155–168.

Stuart, C., Stuart, T. 1998. A field guide to the tracks and signs of southern and east African Wildlife. Southern Books Publishers, Cape Town, 310 pp.

Sues, H.-D., Fraser, N. C., 2010. Triassic life on land: the great transition. New York, Columbia University Press.

Sulej, T., Bronowicz, R., Tałanda, M., Niedźwiedzki, G., 2011. A new dicynodont-archosaur assemblage from the Late Triassic (Carnian) of Poland. Earth & Environmental Science Transactions of The Royal Society of Edinburgh 101, 261–269

Sulej, T., Niedźwiedzki, G., Bronowicz, R., 2012. A new Late Triassic vertebrate fauna with turtles, aetosaurs and coelophysoid dinosaurs from Poland. Journal of Vertebrate Paleontology 32, 1033–1041.

Summons, R.E., Bird, L.R., Gillespie, A.L., Pruss, S.B., Roberts, M., Sessions, A.L., 2013. Lipid biomarkers in ooids from different locations and ages: evidence for a common bacterial flora. Geobiology 11, 420-436.

Szulc, J., Gradziński, M., Lewandowska, A., Heunisch, C., 2006. The Upper Triassic crenogenic

limestones in Upper Silesia (southern Poland) and their paleoenvironmental context. In: Alonso-Zarza, A.M., Tanner, L.H., (Eds.), Paleoenvironmental Record and Applications of Calcretes and Palustrine Carbonates. Geological Society of America Special Paper 416, 133–151.

Świło, M., 2010a. Znaleziska szczątków rekinów ze stanowiska Lipie Śląskie, in Materiały do II Konferencji "Młodzi w Paleontologii". Warszawa, Instytut Paleobiologii PAN, p. 14.

Świło, M., 2010b. Szczątki rekinów triasowych na Śląsku, ich użyteczność w stratygrafii i paleoekologii. Unpublished M.Sc. thesis. Wydział Nauk o Ziemi i Kształtowania Środowiska, Uniwersytet Wrocławski, Wrocław, Poland, 59 p.

Świło, M., 2010c. Znaleziska szczątków rekinów z Lipia Śląskiego In: Zatoń, M., Krawczyński, W., Salamon, M., Bodzioch, A. (Eds.), "Kopalne biocenozy w czasie i przestrzeni". XI Konferencja Naukowa Sekcji Paleontologicznej Polskiego Towarzystwa Geologicznego, Żarki–Letnisko, 13-16 września 2010. Wydział Nauk o Ziemi UŚ, p. 84.

Świło, M., Kowalski, J., 2011. Mikroskamieniałości kręgowców z Lipia Śląskiego. In: Materiały do III Konferencji "Młodzi w Paleontologii". Instytut Botaniki Polskiej Akademii Nauk, Kraków, p. 11.

Świło, M., Niedźwiedzki, G., Sulej, T., 2014. Mammal-like tooth from the Late Triassic of Poland. Acta Palaeontologica Polonica 59, 815–820.

Thiel, V., Blumberg, M., Kiel, S., Leefmann, T., Liebenau, K., Lingren, J., Sjövall, P., Treude, T., Zilla, T., 2014. Occurrence and fate of fatty acyl biomarkers in an ancient whale bone (Oligocene, El Cien Formation, Mexico). Organic Geochemistry 68, 71–81.

Thulborn, A.T., 1991. Morphology, preservation and palaeobiological significance of dinosaur coprolites. Palaeogeography, Palaeoclimatology, Palaeoecology 83, 341–366.

Van Geel, B. Aptroot, A. Baittinger, C., Birks, H.H., Bull, I.D., Cross, H.B., Evershed, R.P., Gravendeel, B., Kompanje, E.J.O., Kuperus, P., Mol, D., Nierop, K.G.J., Pals, J.P.,

Tikhonov, A.N., van Reenen, G., van Tienderen, P.H., 2008. The ecological implications of a Yakutian mammoth's last meal. Quaternary Research 69, 361–376.

Veiga, P., Juste, C., Lepercq, P., Saunier, K., Béguet, F., Gérard, P., 2005. Correlation between faecal microbial community structure and cholesterol-to-coprostanol conversion in the human gut. FEMS Microbiology Letters 242: 81–86.

Wawrzyniak, Z., 2010a. Tafonomia późnotriasowej flory z Lipia Śląskiego. In: Materiały do II Konferencji "Młodzi w Paleontologii". Warszawa, Instytut Paleobiologii PAN, p. 16.

Wawrzyniak, Z., 2010b. Późnotriasowa flora z Lipia Śląskiego. Unpublished M.Sc. thesis. Wydział Nauk o Ziemi, Uniwersytet Śląski, Sosnowiec, Poland, 76 pp.

Wawrzyniak, Z., 2010c. Późnotriasowe kutykule z Lipia Śląskiego k. Lublińca. In: Zatoń, M., Krawczyński, W., Salamon, M., Bodzioch, A. (Eds.), "Kopalne biocenozy w czasie i przestrzeni". XI Konferencja Naukowa Sekcji Paleontologicznej Polskiego Towarzystwa Geologicznego, Żarki–Letnisko, 13-16 września 2010. Wydział Nauk o Ziemi UŚ, p. 85.

Wawrzyniak, Z., 2011. The Upper Triassic cuticles from Lipie Śląskie (South Poland). In: Bąk, M., Kaminski, M.A., Waśkowska, A., (Eds.), Integrating microfossil records from the oceans and epicontinental seas. Grzybowski Foundation Special Publication 17, 140–141.

Wawrzyniak, Z., Ziaja, J., 2009. Wstepne wyniki badan gornotriasowej makroflory Lipia Śląskiego, Polska. Geologia 35, 105–106.

Wood, G.D., Gabriel, A.M., Lawson, J.C., 1996. Palynological techniques—processing and microscopy. In: Jansonius, J., McGregor, D.C., (Eds.), Palynology: Principles and Applications 1, 29–50.

Wood, J.R., Wilmshurst, J.M., 2014. Late Quaternary terrestrial vertebrate coprolites from New Zealand. Quaternary Science Reviews 98, 1–12.

Yates, A.M., Neumann, F.H., Hancox, P.J., 2012. The earliest post-Paleozoic freshwater bivalves preserved in coprolites from the Karoo Basin, South Africa. PLoS ONE 7(2):, e30228. http://dx.doi.org/10.1371/journal.pone.0030228.

Zatoń, M., Rakociński, M., 2014. Coprolite evidence for carnivorous predation in a Late Devonian pelagic environment of southern Laurussia. Palaeogeography, Palaeoclimatology, Palaeoecology 394, 1–11.

Figure and table captions:

Figure 1. Geological sketch-map showing the localization of the bone- and coprolite-bearing sites at Poręba and Lisowice (adopted from Niedźwiedzki et al. 2014).

Figure 2. Lithostratigraphic section of deposits exposed at the Poręba clay-pit (adopted from Niedźwiedzki et al. 2014).

Figure 3. Sketch-drawing of the faunal assemblage of the Poręba site. A - Large predatory archosaur (rauisuchian or predatory dinosaur), b - neotheropod dinosaur, c - theropod dinosaur Herrerasauridae indet., d - large temnospondyl amphibian, e - hybodont shark, f - dipnoan fish *Ptychoceratodus* sp., g - actinopterygian fish, h - aetosaur, i - turtle *Proterochersis* sp., j - dinosauriform Silesauridae indet.

Figure 4. Lithostratigraphic section of deposits exposed at the Lisowice clay-pit (adopted from Pieńkowski et al. 2014).

Figure 5. Sketch-drawing of the faunal assemblage of the Lisowice site. A - large, early predatory dinosaur *Smok wawelski*, b - large temnospondyl amphibian *Cyclotosaurus* sp., c – small theropod dinosaur Theropoda indet., d - temnospondyl amphibian *Gerrothorax* sp., e - small ‘rauisuchian’ Poposauridae indet., f - small diapsid Choristodera indet., g - hybodont shark, h - coelacanth fish, i - dipnoan fish *Ptychoceratodus* sp., j - actinopterygian fish, k - large dicynodont Kannemeyeriiformes indet., l - small archosauromorph Rhynchosauria indet., m - dinosauriform Silesauridae indet., n - small lepidosaur Sphenodontia indet., o - pterosaur, p - mammaliaform *Hallautherium* sp.

Figure 6. Examples of Upper Triassic coprolites studied from Poland. A, C, E-F, H-I. Coprolites of the morphotype 2. B, D, G, J. Coprolites of the morphotype 1. K. Coprolite of the morphotype 3. A. Coprolite from Poręba. B-K. Coprolites from Lisowice. Scale bars equal 1 cm.

Figure 7. ESEM photomicrographs of coccoid microstructures composing the phosphatic groundmass of the coprolites investigated. A. COP01, Poręba. B. COP04a, Lisowice. C. COP05, Lisowice. D. COP14, Lisowice.

Figure 8. TEM and STXM analyses of the coccoid structures in the FIB foils obtained from the Late Triassic coprolite from Lisowice (sample COP04a). A. General view of FIB foil 1 in TEM bright field mode. Numerous coccoid structures are observed as empty or filled spheres. B-D. Close-up of coccoid structures (FIB foil #1 and 2) showing a completely filled, small-grained coccoid structure (B) with a denser wall (arrows); an empty structure with a thick wall (C), and a structure with francolite crystals inside (D). E-G. Energy dispersive X-ray spectrometry (EDXS) maps of Ca, P and Ga. Ca and P are homogeneously distributed. Ga is preferentially located in holes. H. Typical EDXS spectrum of francolite. A Ca/P ratio of ~1.6 is derived from EDXS analyses. I. X-ray absorption near edge structure (XANES) spectrum at the Ca L2,3 edges obtained by STXM on francolite. Peaks at 347.2, 348.3, 348.7, 349.3, 351.6 and 352.6 are consistent with francolite. J. XANES spectrum at the C K-edge obtained by STXM on francolite. Peaks at 290.3 and 300.8 eV are characteristics of carbonate functional groups.

Figure 9. XRD patterns of nine coprolite samples (a) and host rock sample (b). A - apatite, C – calcite, D – dolomite, I-illite and mica, K – kaolinite, Q – quartz, Sm - smectite. The angular distance between the 410-00 apatite peaks is used to determine the carbonate content.

Figure 10. Examples of coprofabrics in thin-sections of the coprolites investigated. A-B. Transmitted-light microscope views of coprofabrics consisting of microcrystalline apatitic mucosal folding and sparry calcite between the folds, morphotype 2, specimens COP01 (Poręba) and COP14 (Lisowice), respectively. C. Transmitted-light microscope view of microcrystalline apatite groundmass with sparry calcitic grains and dispersed plant tissues, morphotype 2, specimen COP16 (Poręba). D. Reflected-light microscope view of strongly pyritized (light places) coprolite of the morphotype 3, specimen COP11 (Lisowice).

Figure 11. Total ion current (TIC) of the saturated hydrocarbons fraction of two Upper Triassic coprolites from Lisowice. Numbers over the peaks identify individual carbon number homologues. Pr - pristane, Ph - phytane, *N*Pr - nor-pristane.

Figure 12. Total ion current (TIC) of the polar fraction (as TMS derivatives) of the sample COP09 (Lisowice).

Figure 13. Transmitted-light microscope photographs of thin-sections showing the bone and scale remains preserved in Upper Triassic coprolites. A-B. Flat and poorly vascularized long bones showing the characteristic rounded ends. C. Highly vascularized bone element with digested outer surface. D. Positions of bone elements inside the fecal groundmass. E. Bone fragments showing damages. F. Fish scale showing amorphous, thick enamel layer and dentine with numerous dentinal tubules. A. COP14, Lisowice, B, D, F. COP06, Lisowice, C. COP16, Poręba, E. COP18, Lisowice.

Figure 14. Transmitted-light microscope photographs of thin-sections showing the bone, tooth and fibrous remains preserved in Upper Triassic coprolites. A-B. Highly degraded bone fragments. C. Transverse section of a tooth showing a thin layer of dentine surrounding a large pulp cavity. D.

Poorly preserved fibrous elements. A-B. COP12, Lisowice, C. COP01, Poręba, D. COP14, Lisowice.

Figure 15. Transmitted-light microscope photographs of thin-sections showing the bone and fibrous remains preserved in Upper Triassic coprolites. A. Association of bone fragments and tightly packed fibrous elements. B. Highly degraded bone fragments. C. Small bone with calcified cartilage of the bony trabeculae. D-F. Skeletal elements with record microbial attack (bacteria or fungi). A, D-E. COP06, Lisowice, B-C, F. COP14, Lisowice.

Figure 16. Categories and percentage contribution of organic remains present in the coprolites studied.

Figure 17. Plant cuticles found in the coprolites studied. A-D. Cuticle type A, very similar to *Lepidopteris ottonis*, COP05, Lisowice. E-F. Cuticle type B, similar to *Podozamites*, COP16, Poręba. G-I. closely unidentifiable cuticle type C, COP16, Poręba.

Figure 18. Plant tracheids and cuticle found in the coprolites studied. A-K. Various types and differently preserved woody tracheids. A, C, E-K, COP16, Poręba; B, D. COP10, Lisowice. L. A tissue infested by fungi, COP16, Poręba. M. Closely unidentified cuticle type D, COP08, Lisowice.

Figure 19. Various types of arthropod cuticle derived from coprolites. A-B. COP16, Poręba, C. COP01, Poręba, D. COP08, Lisowice.

Table 1. Data on sample number, provenance, kind of morphotype and methodologies used for the study of the Upper Triassic coprolites from Poland.

Table 2. Results of major elemental analysis using FUS-ICP of selected Upper Triassic coprolites and host rock (shaded area).

Table 3. Results of XRD analysis of selected Upper Triassic coprolites and host rock (shaded area).

Table 4. Total organic carbon (TOC), total sulphur (TS) and carbonate content (CC) in the selected Upper Triassic coprolites.

Table 5. Polar compounds detected in selected Upper Triassic coprolites as an TMS derivatives. Abundances normalized to $C_{16:0}$ fatty acid, the most abundant lipid.

Electronic Supplementary Material

ESM Fig. 1. Plot showing correlation of chemical elements present in apatite using the data obtained by EMP analysis. The geochemical trends for apatites in bone remains (A and B) and apatite groundmass (C) are: increase of the SO_2 content inside apatite building the interior of bone fragments (black points, A), increase in the P_2O_5 content of apatite building the marginal zones of bone fragments (grey and violet points, A-B), relatively low content of P_2O_5 in the apatite groundmass (yellow points, C).

Figure 1
Click here to download high resolution image

Figure 2

Click here to download high resolution image

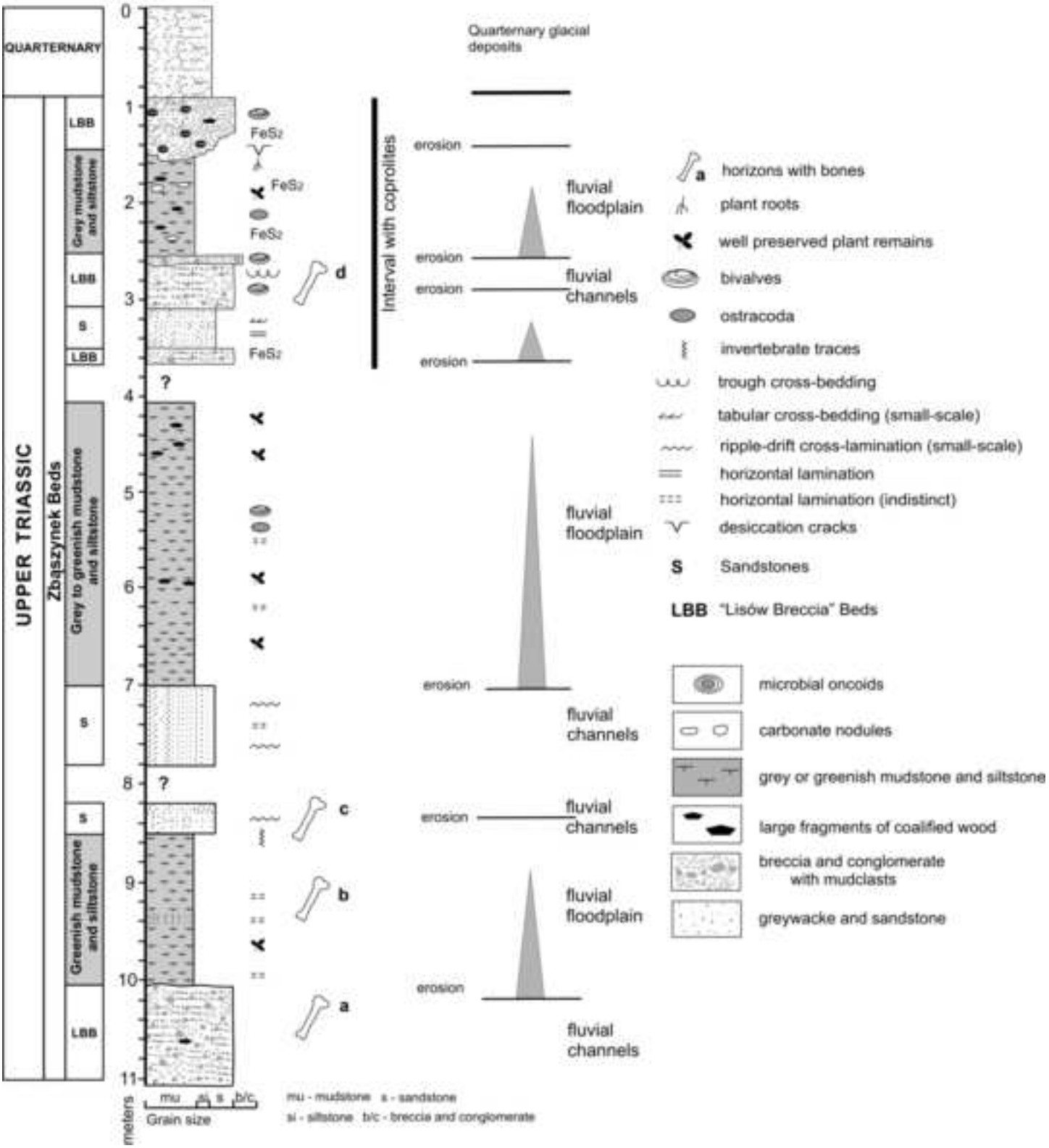

Figure 3
Click here to download high resolution image

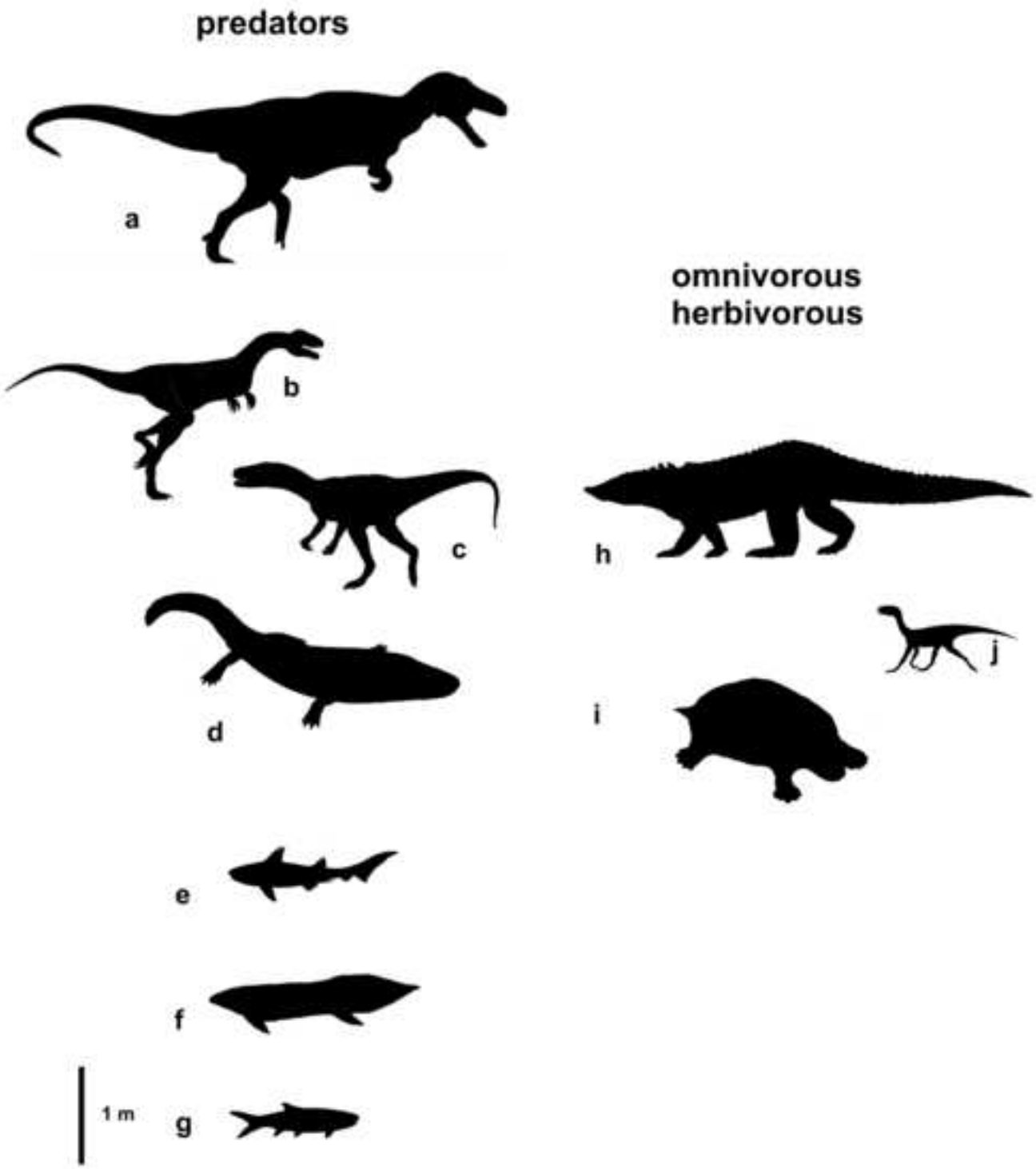

Figure 4

Click here to download high resolution image

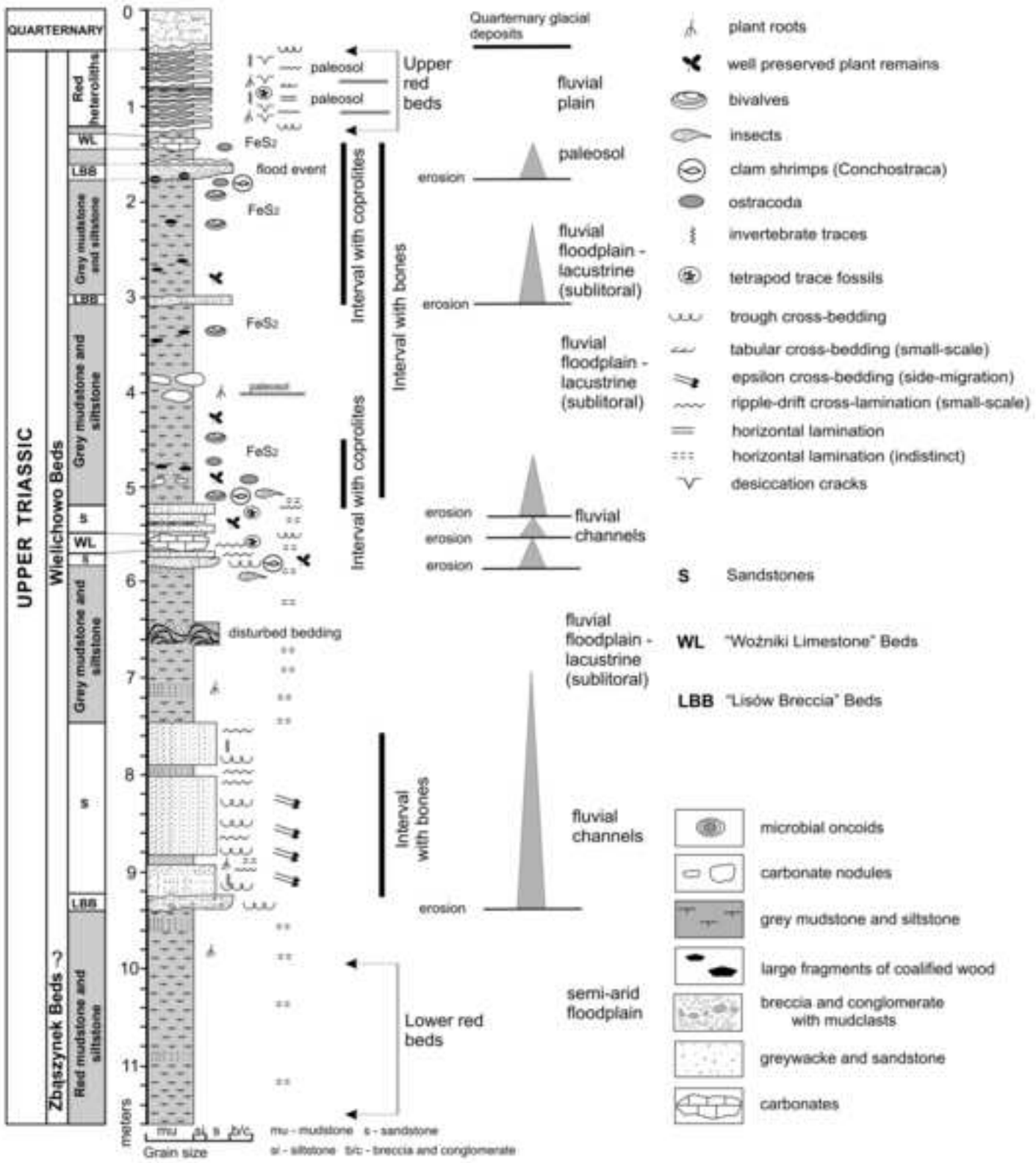

Figure 5
Click here to download high resolution image

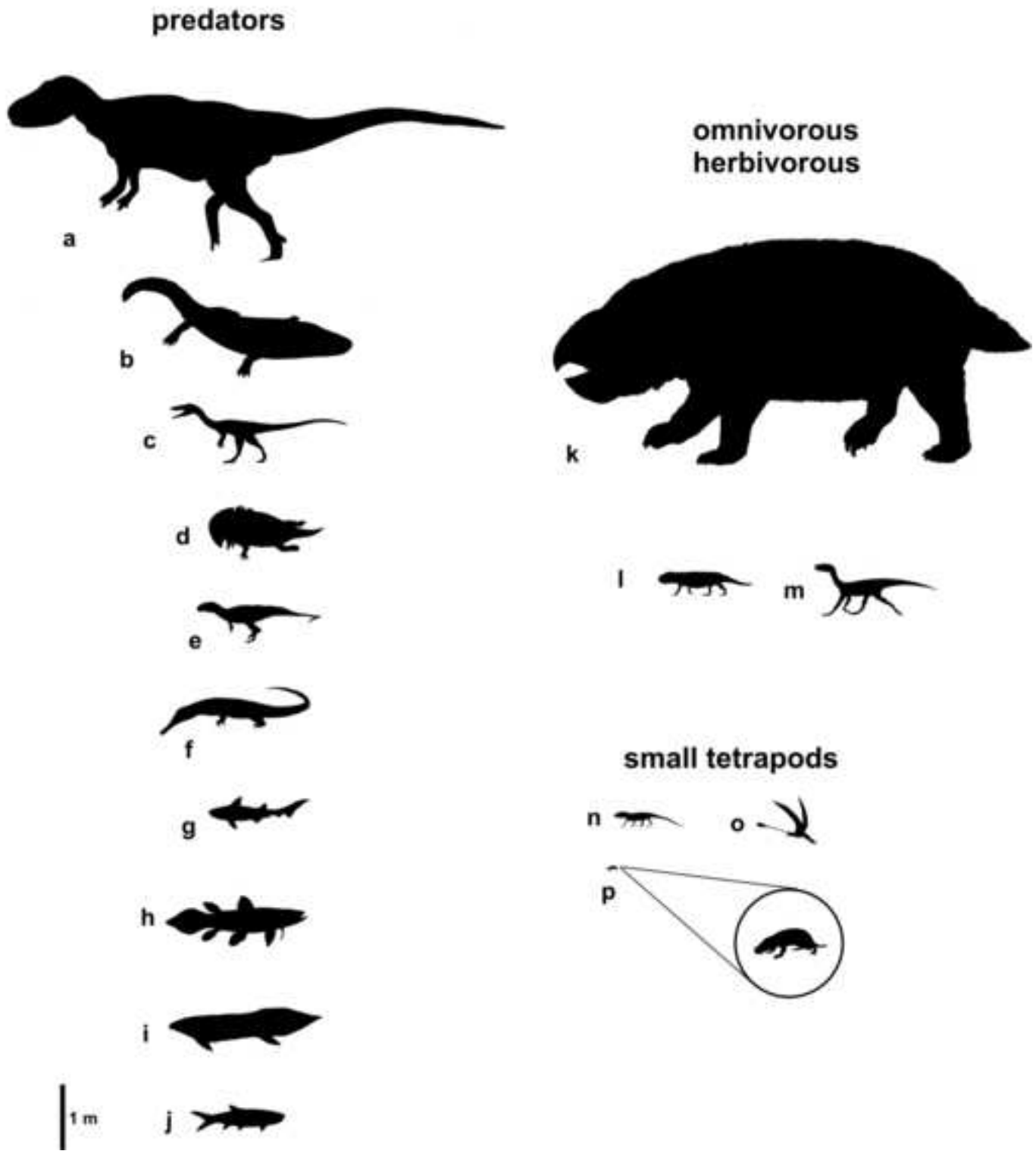

Figure 6
Click here to download high resolution image

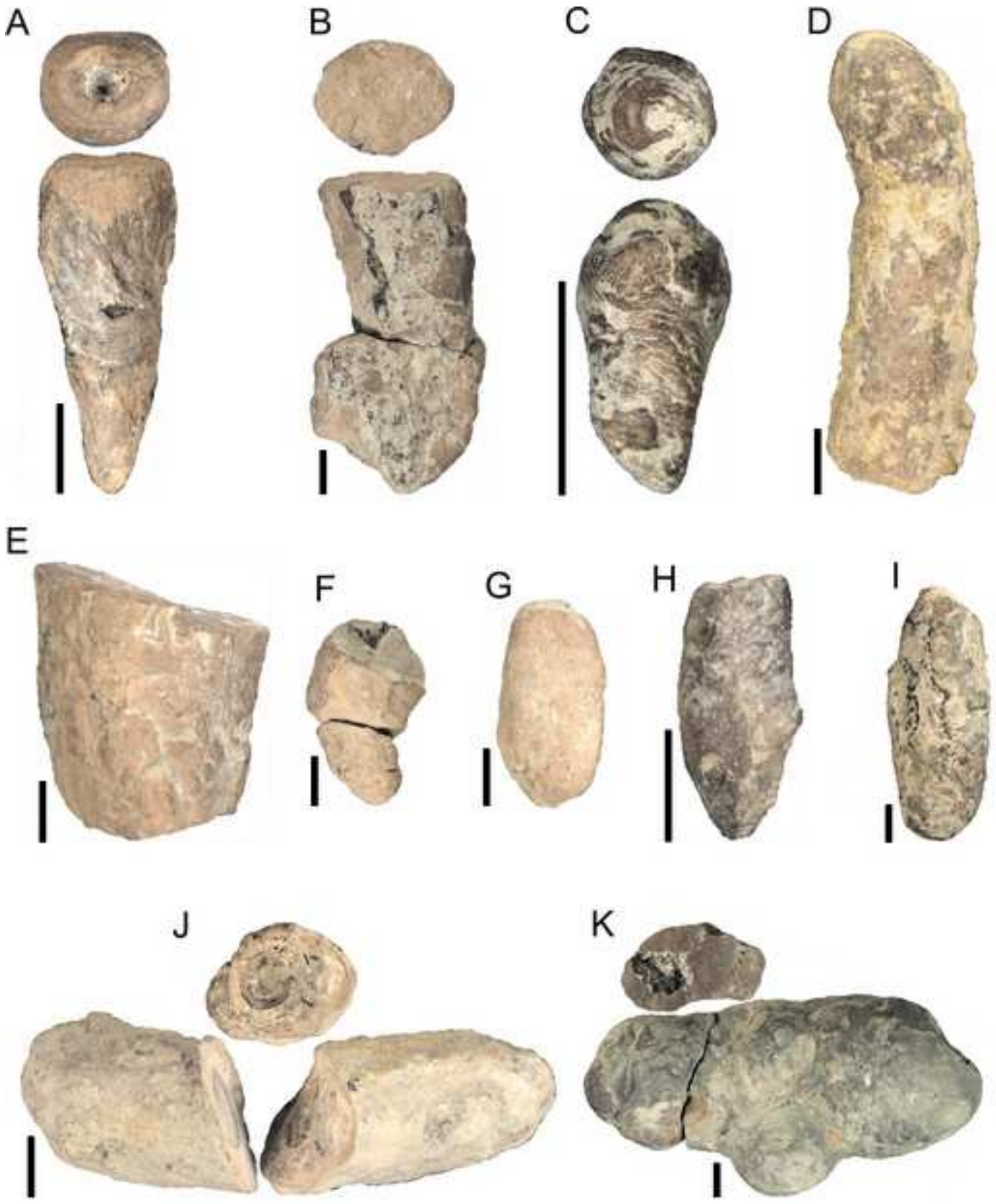

Figure 7
Click here to download high resolution image

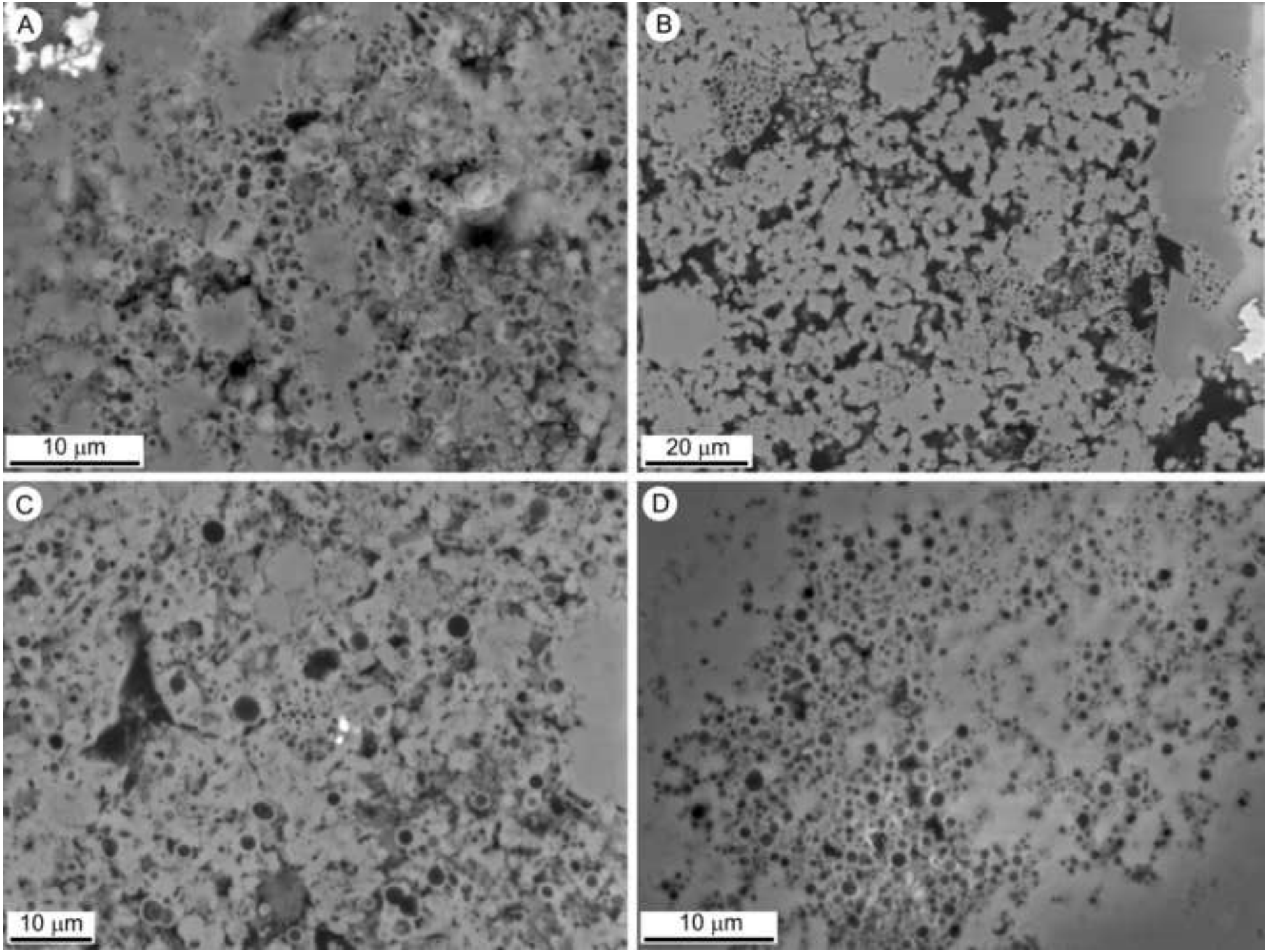

Figure 8
Click here to download high resolution image

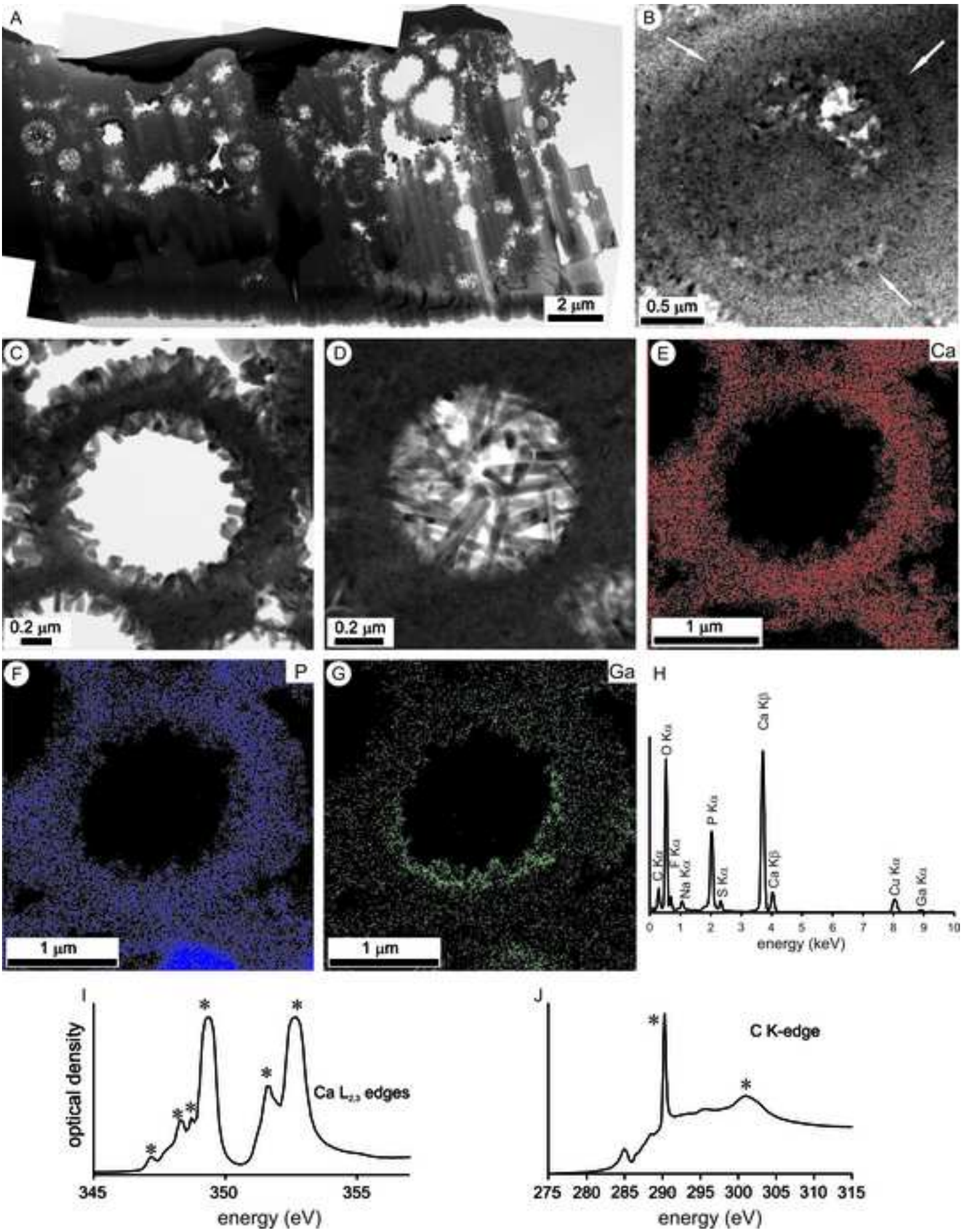

Figure 9

Click here to download high resolution image

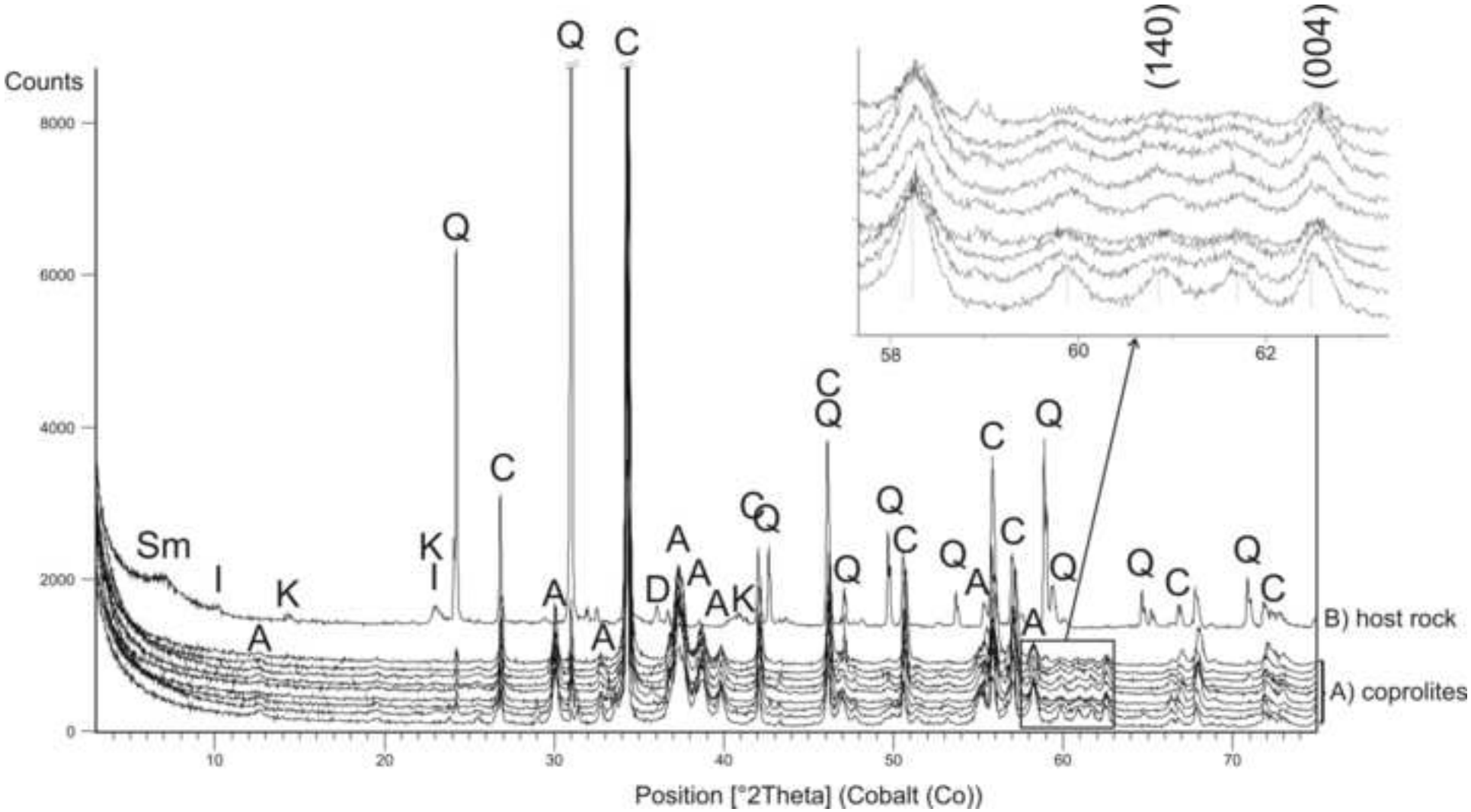

Figure 10

Click here to download high resolution image

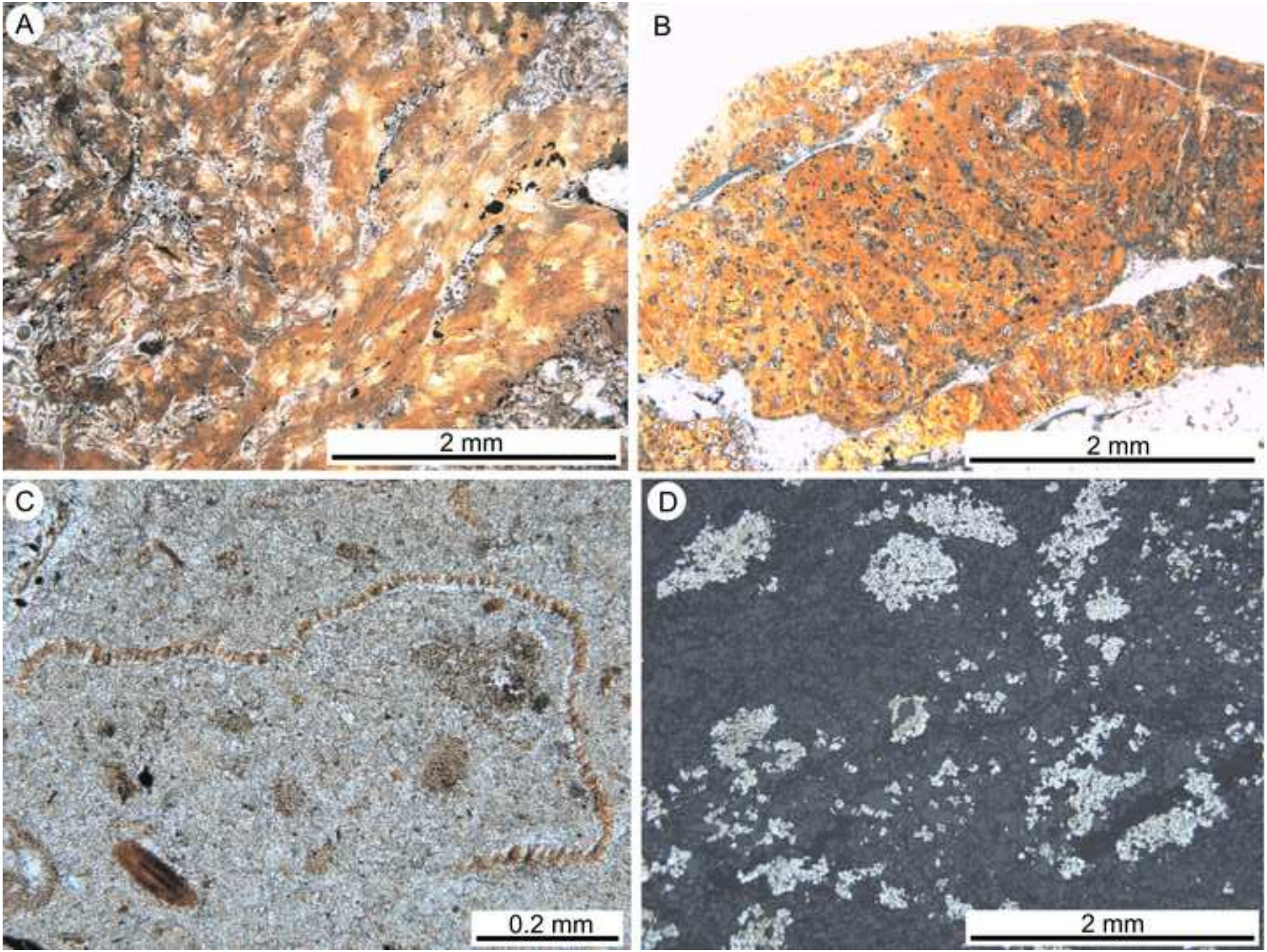

Figure 11
Click here to download high resolution image

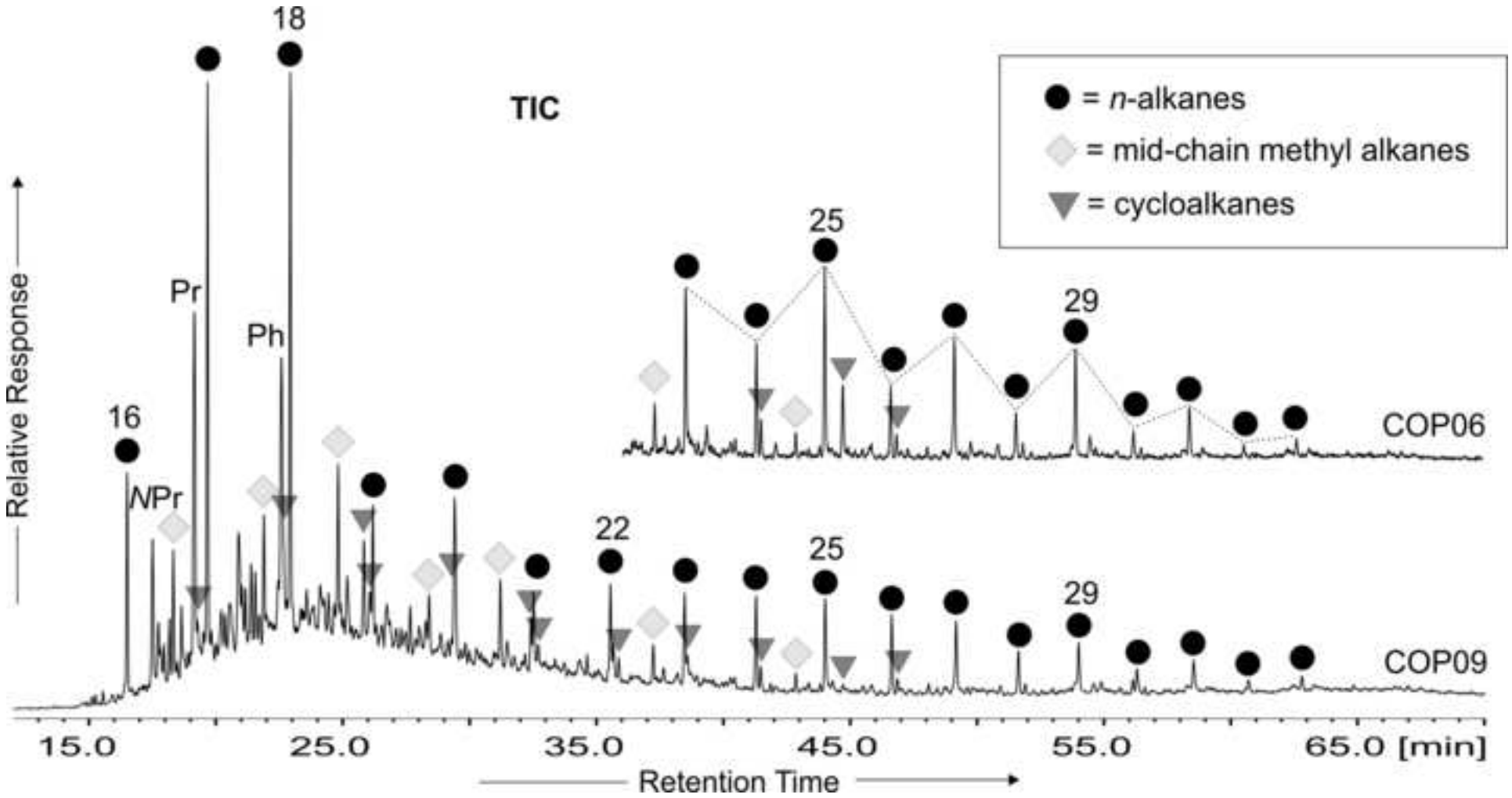

Figure 12

Click here to download high resolution image

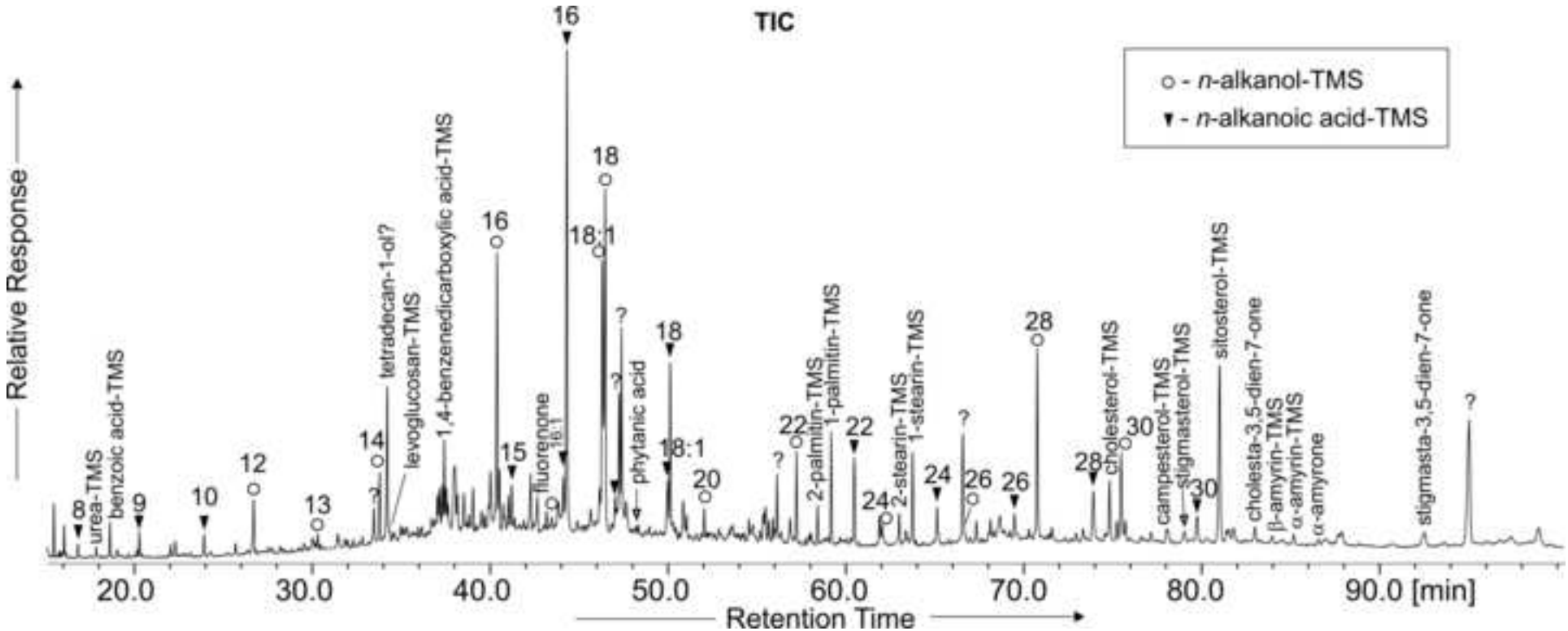

Figure 13
Click here to download high resolution image

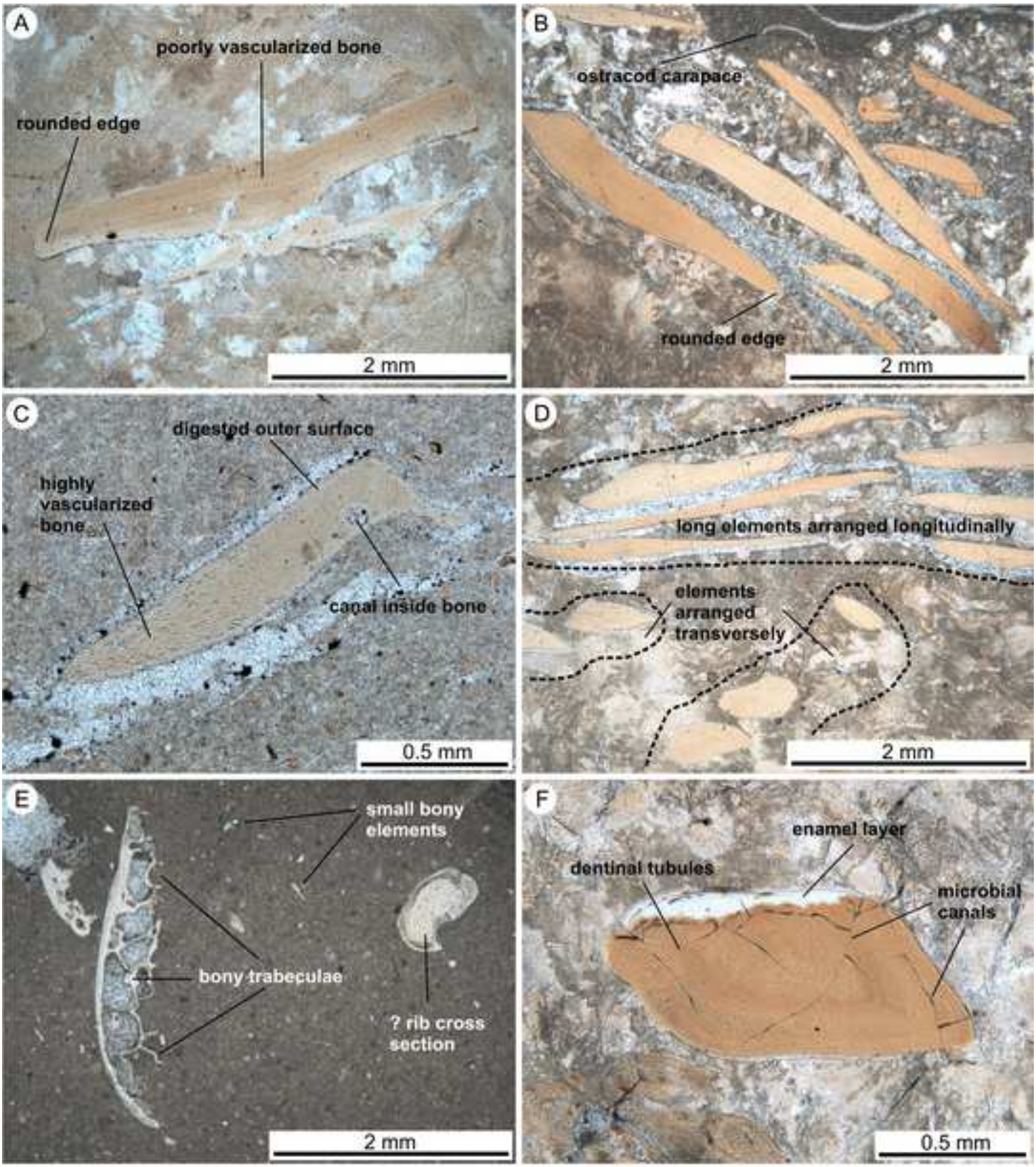

Figure 14
Click here to download high resolution image

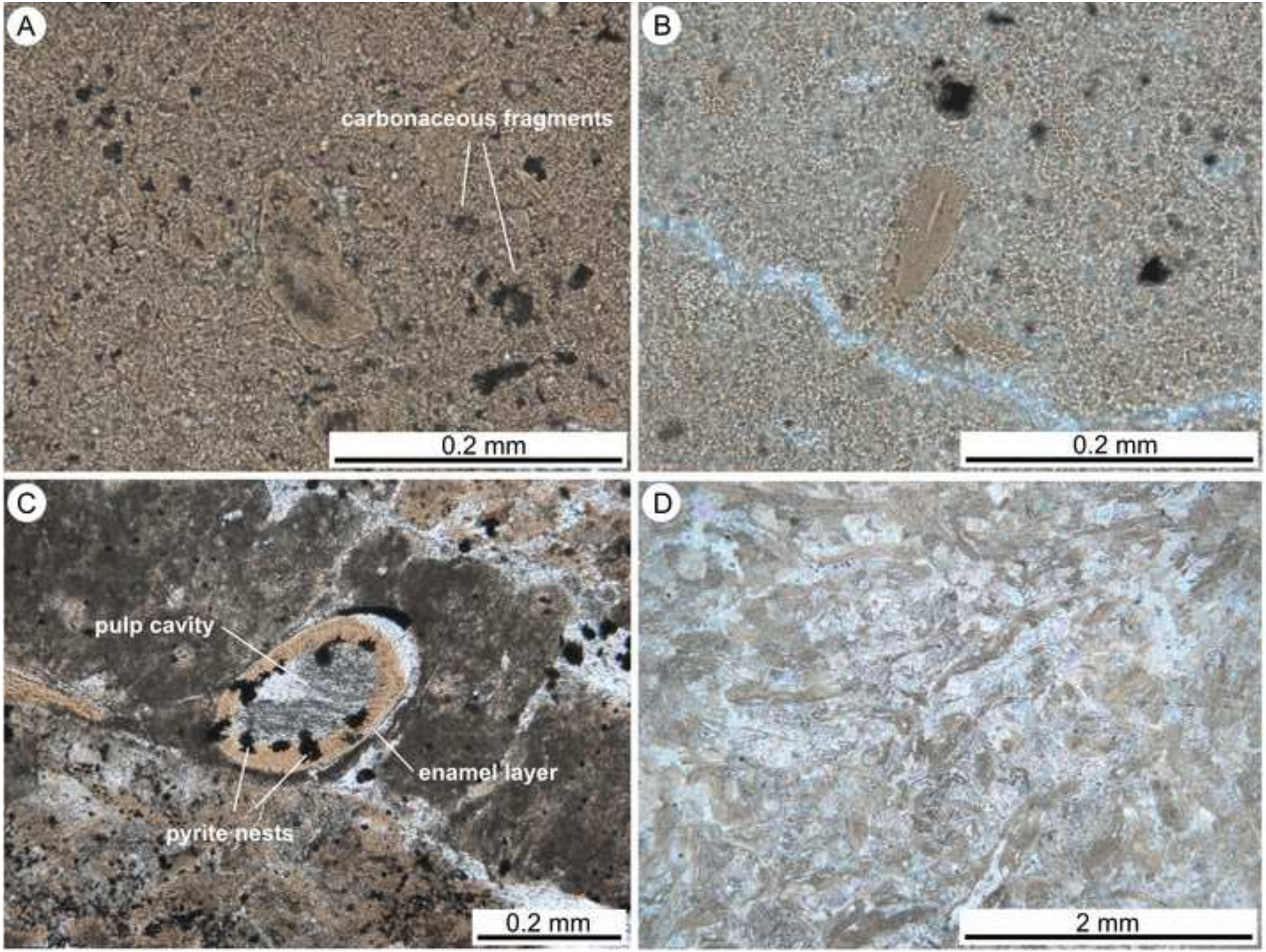

Figure 15
Click here to download high resolution image

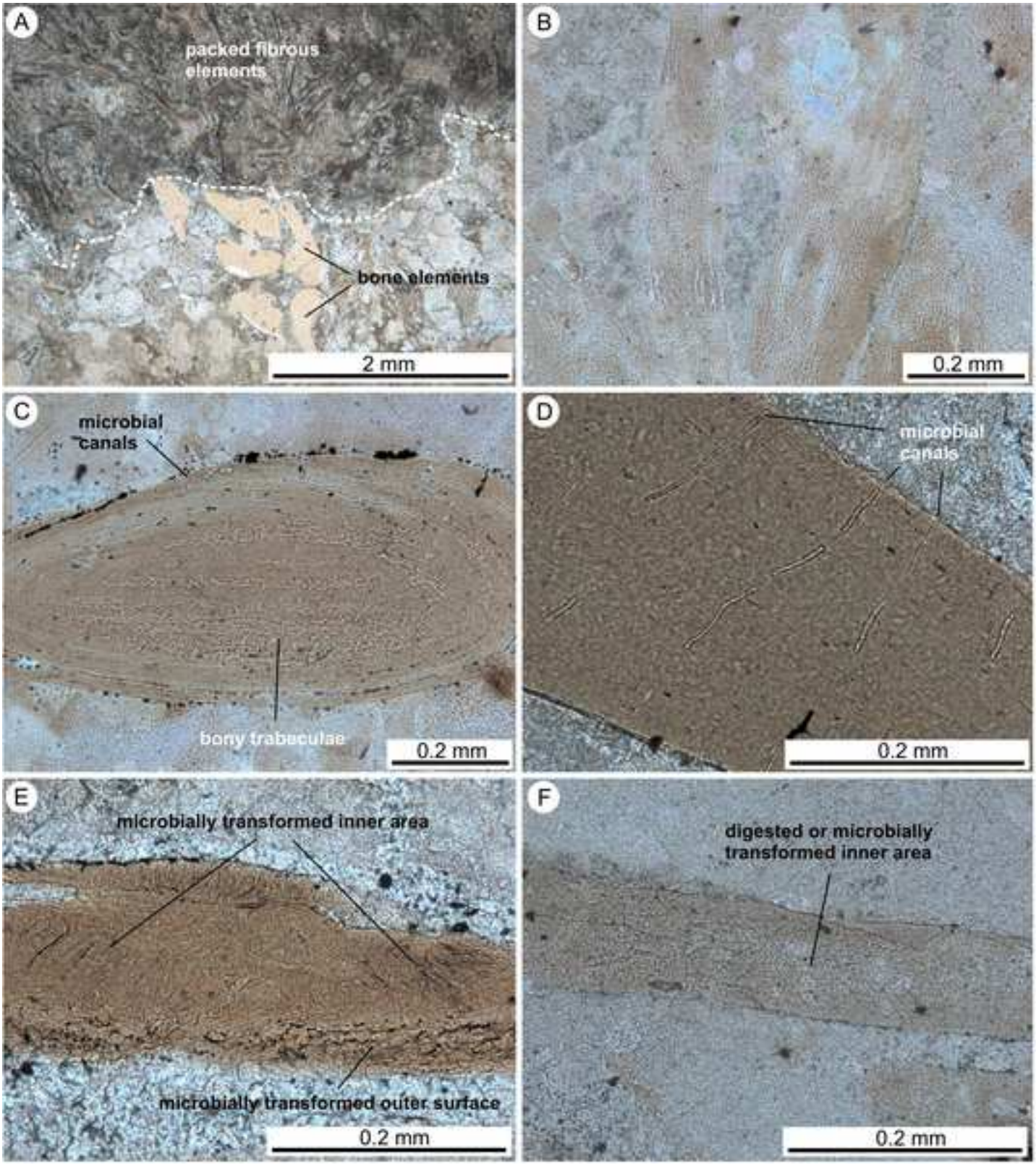

Figure 16

Click here to download high resolution image

	Category	I			II			III	IV		
	Sample/COP-	05	08	10	07	09	18	16	01	02	06
	Plant cuticles	22,5	18	22	3,5	8,5	2	7,5	0	0	0,5
	Plant tracheids	15	14	12	4	8	10	34	0	1	0
	Miospores	6,5	8,5	3,5	14	0	1	16,5	0	0	1
	Animal cuticles	0	0	0,5	0	0	0	0,5	1	0	0
	Brown debris	36,5	33	58,5	72,5	42,5	59	37	34	51,5	55
	Black debris	19,5	26,5	4,5	6	41	27,5	4,5	65	47,5	43,5
	Fraction [mm]	>2		1-0,5		3-5			< 0,5		

%

Figure 17
Click here to download high resolution image

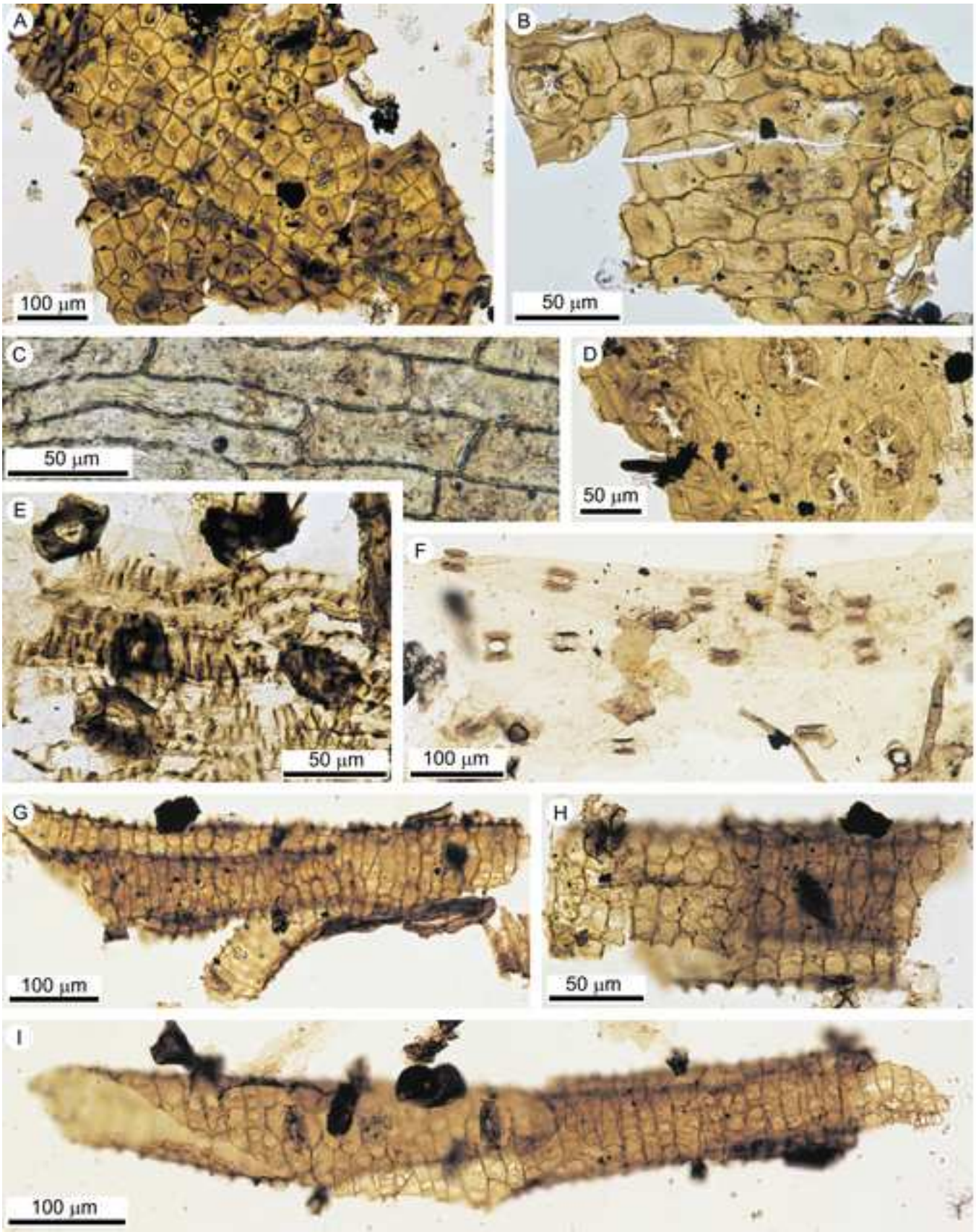

Figure 18
Click here to download high resolution image

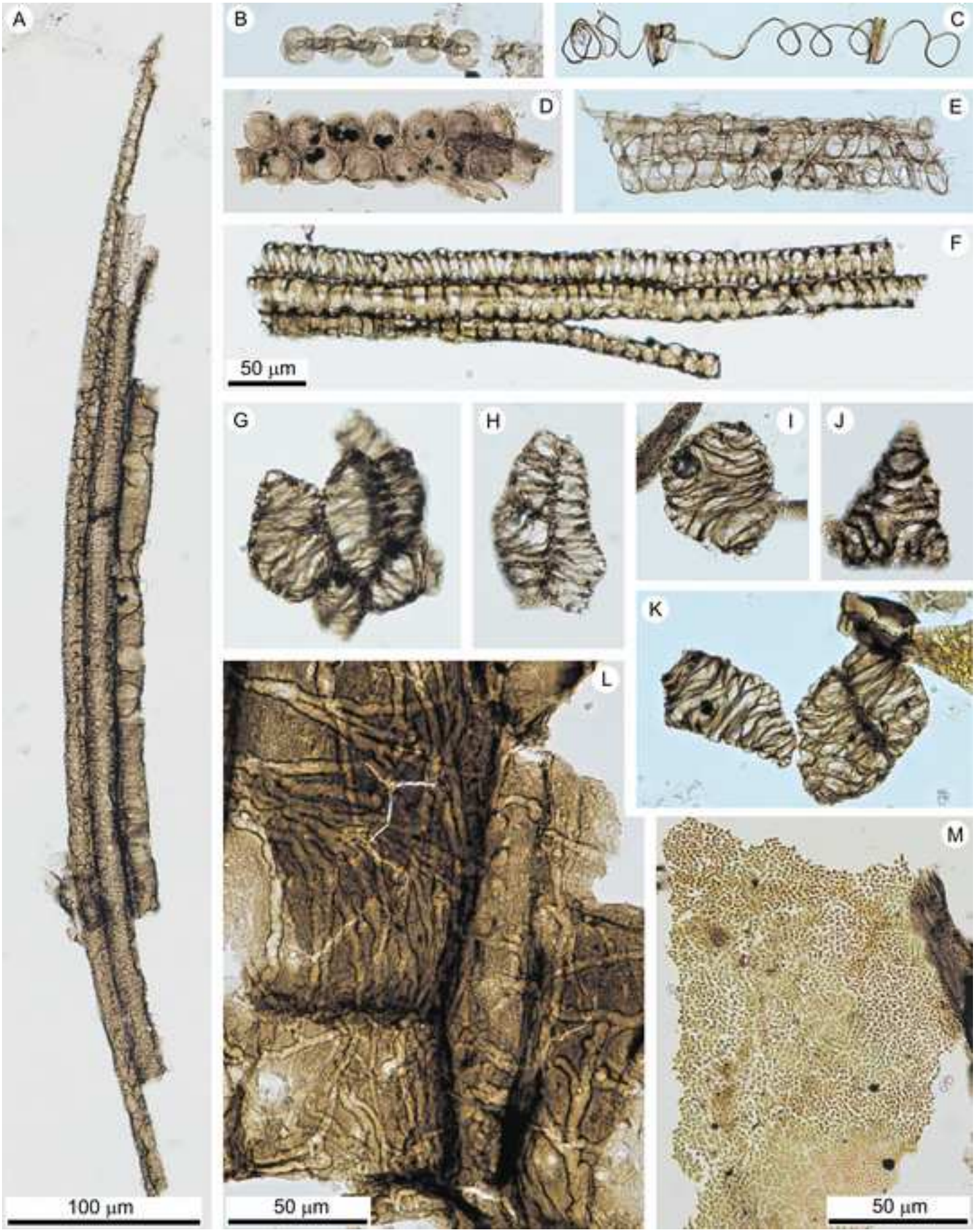

Figure 19
Click here to download high resolution image

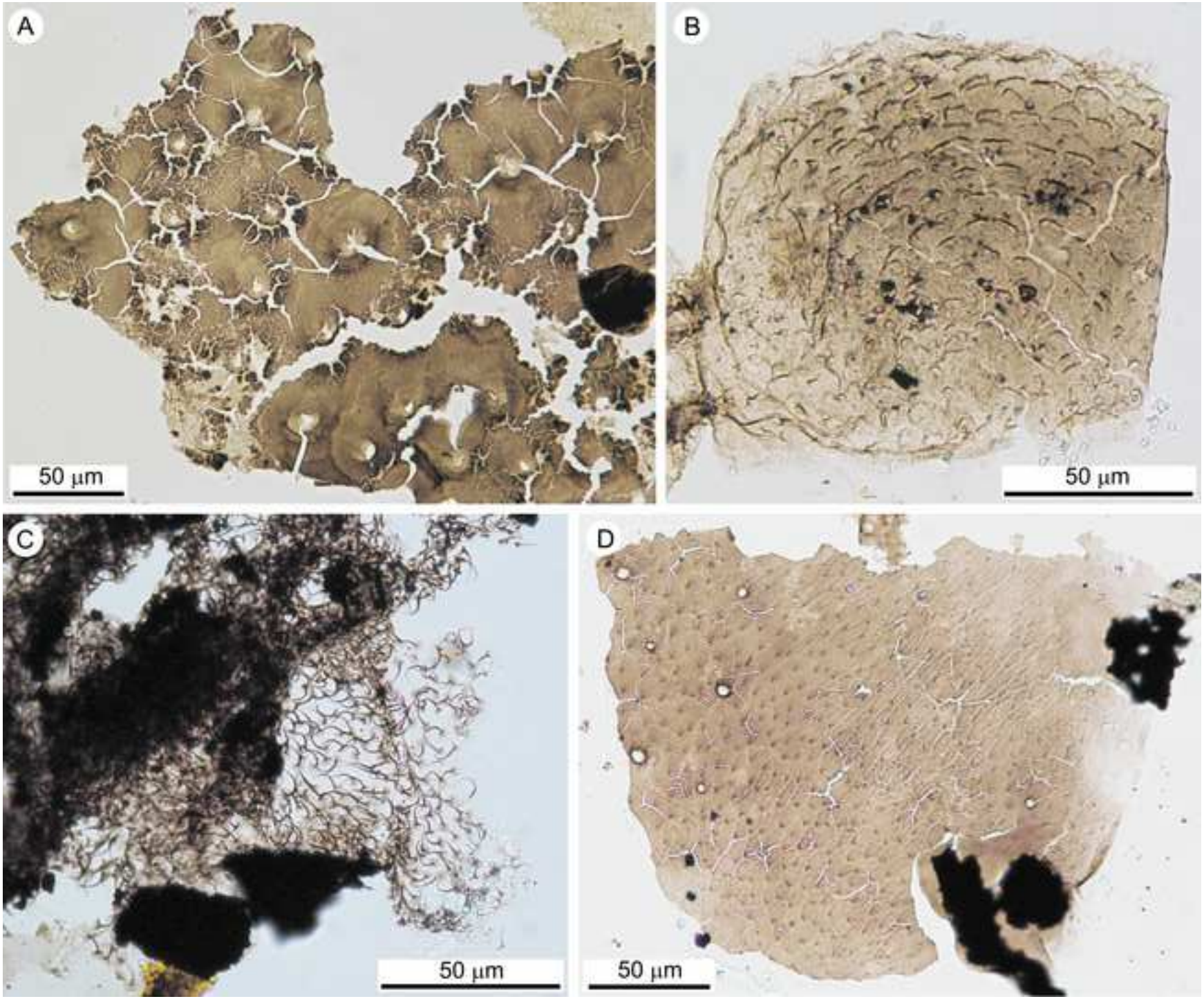

ESM Figure 1
Click here to download high resolution image

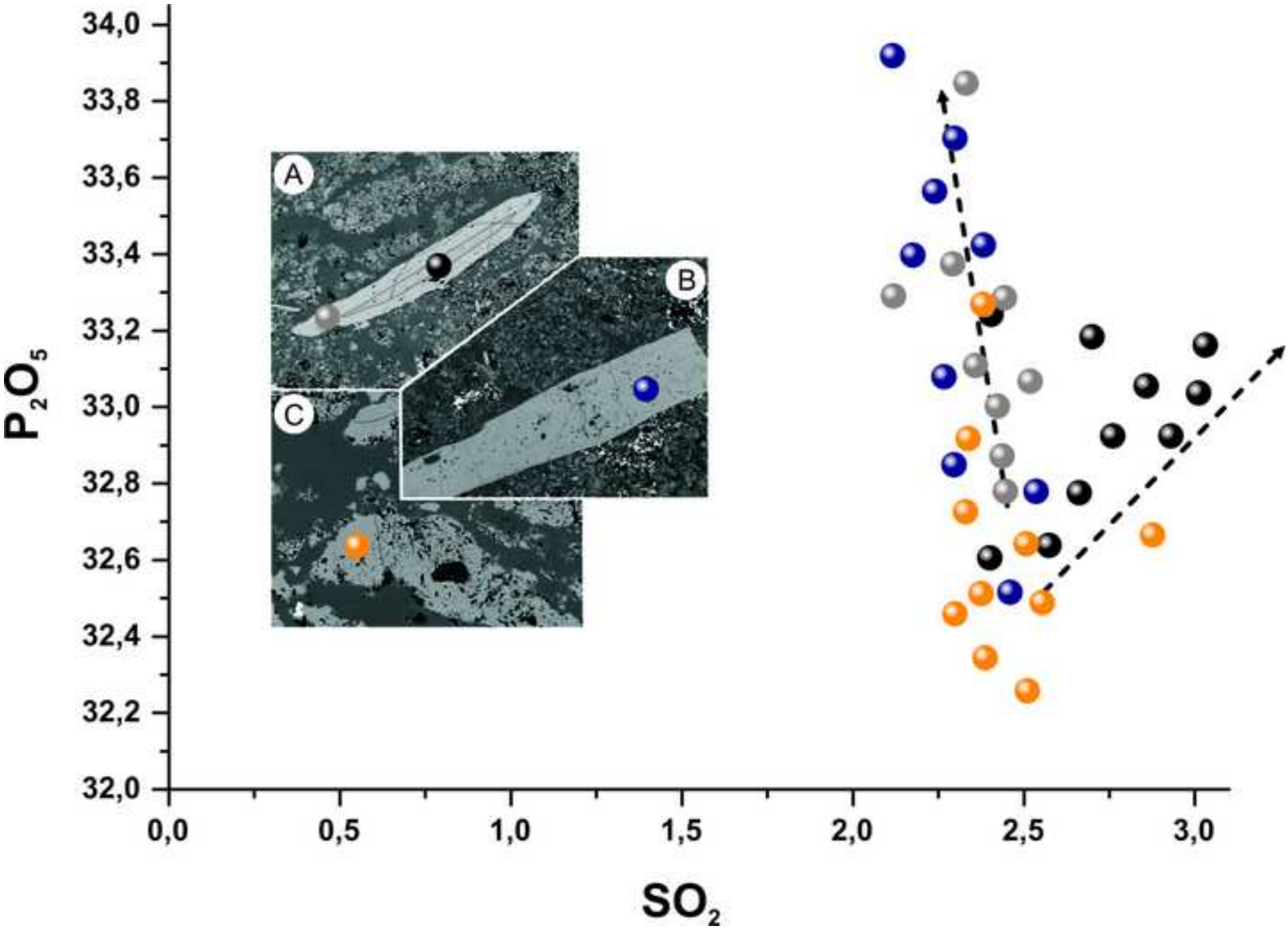

Table 1

Click here to download Table: Table 1.doc

sample number/locality	morphotype	analyses applied
ZPAL V.39/372 COP01/Poręba	morphotype 2	transmitted-light microscopy, SEM, palynology, TOC and TS,
ZPAL V.33/1270 COP02/Lisowice	morphotype 1 (fragmentary)	palynology
ZPAL V.33/1270 COP03/Lisowice	morphotype 2	SEM, TOC and TS
ZPAL V.33/1270 COP04a/Lisowice	morphotype 1	transmitted-light microscopy, SEM, TEM, STXM, inorganic geochemistry, XRD, TOC and TS
ZPAL V.33/1270 COP05/Lisowice	morphotype 1	transmitted-light microscopy, SEM, palynology, inorganic geochemistry, XRD, TOC and TS, biomarkers
ZPAL V.33/1270 COP06/Lisowice	morphotype 1	transmitted-light microscopy, palynology, inorganic geochemistry, XRD, TOC and TS, biomarkers
ZPAL V.33/1270 COP07/Lisowice	morphotype 1	transmitted-light microscopy, palynology, inorganic geochemistry, XRD, TOC and TS
ZPAL V.33/1270 COP08/Lisowice	morphotype 2	transmitted-light microscopy, SEM, palynology, inorganic geochemistry, XRD
ZPAL V.33/1270 COP09/Lisowice	morphotype 2	SEM, palynology, inorganic geochemistry, XRD, biomarkers
ZPAL V.33/1270 COP10/Lisowice	morphotype 1	transmitted-light microscopy, SEM, palynology, inorganic geochemistry, XRD
ZPAL V.33/1270 COP11/Lisowice	morphotype 3 (pyritized)	transmitted-light microscopy
ZPAL V.33/1270 COP12/Lisowice	morphotype 3	transmitted-light microscopy
ZPAL V.33/1270 COP13/Lisowice	morphotype 1	transmitted-light microscopy
ZPAL V.33/1270 COP14/Lisowice	morphotype 2	transmitted-light microscopy, SEM, TOC and TS, biomarkers
ZPAL V.33/1270 COP15/Lisowice	morphotype 3 (pyritized)	transmitted-light microscopy
ZPAL V.39/372 COP16/Poręba	morphotype 2	transmitted-light microscopy, SEM, palynology, inorganic geochemistry, XRD, TOC and TS, biomarkers
ZPAL V.33/1270 COP18/Lisowice	morphotype 2	transmitted-light microscopy, SEM, palynology, inorganic geochemistry, XRD, biomarkers
ZPAL V.33/1270 COP19/Lisowice	morphotype 2	transmitted-light microscopy

Table 2

Click here to download Table: Table 2.docx

Analyte Symbol	**SiO_2**	**Al_2O_3**	**Fe_2O_3**	**MnO**	**MgO**	**CaO**	**Na_2O**	**K_2O**	**P_2O_5**	**TiO_2**	**Sum**
Unit Symbol	wt. %	wt. %	wt. %	wt. %	wt. %	wt. %	wt. %	wt. %	wt. %	wt. %	wt. %
Detection Limit	0.01	0.01	0.01	0.001	0.01	0.01	0.01	0.01	0.01	0.001	0.01
Analysis Method	FUS-ICP	FUS-ICP	FUS-ICP	FUS-ICP	FUS-ICP	FUS-ICP	FUS-ICP	FUS-ICP	FUS-ICP	FUS-ICP	FUS-ICP
COP 04a	1,17	0,19	0,41	0,143	0,24	48,73	1,14	0,04	20,3	0,012	91,7
COP 04b	49,03	4,23	1,3	0,119	1,28	23,13	0,33	0,83	0,11	0,366	100,2
COP 05	6,91	1,73	0,95	0,12	0,52	43,19	1	0,26	19,58	0,07	87,47
COP 06	3,04	0,9	0,8	0,511	0,64	50,47	0,13	0,18	9,1	0,045	93,75
COP 07	2,41	0,56	2,48	1,017	0,43	49,99	0,32	0,11	11,73	0,043	96,36
COP 08	1,92	0,62	1,13	0,214	0,38	49,15	0,86	0,13	17,97	0,033	93,17
COP 09	7,16	1,06	0,55	0,15	0,47	44,99	0,91	0,2	20,21	0,089	92,96
COP 10	0,71	0,24	0,21	0,208	0,36	49,7	0,84	0,04	17,91	0,011	87,95
COP 16	3,01	0,68	0,79	0,438	0,77	49,23	0,13	0,14	10,24	0,042	95,2
COP 18	1,91	0,45	1,54	0,214	0,32	46,81	0,53	0,15	18,5	0,026	89,08

Table 3

Click here to download Table: Table 3.docx

sample	apatite [wt. %]	calcite [wt. %]	barite [wt. %]	quartz [wt. %]	pyrite [wt. %]	dolomite [wt. %]	clay min. [wt. %]	goethite [wt. %]	feldspars [wt. %]
COP04a	48	44	4	2	2	-	-	-	-
COP04b	-	40	-	45	tr	3	8	-	3
COP05	60	25	7	6	2	-	-	-	-
COP06	19	79	-	tr	-	tr	tr	-	-
COP07	32	65	-	2	-	-	-	tr	-
COP08	54	45	-	tr	tr	-	tr	-	-
COP09	68	28	-	4	tr	-	tr	-	-
COP10	55	45	-	tr	-	-	-	-	-
COP16	29	68	-	2	tr	-	tr	-	-
COP18	57	40	-	tr	2	-	-	-	-

Table 4
Click here to download Table: Table 4.docx

Table 1. Total organic carbon (TOC), total sulphur (TS) and carbonate content (CC) in Upper Triassic coprolites.

Samples	**TS**	**TOC**	**CC**
COP1	0,06	**1,16**	58,1
COP3	0,00	**1,31**	30,7
COP04	0,00	**0,68**	45,5
COP05	1,03	**0,99**	25,1
COP06	0,00	**0,55**	78,2
COP07	0,00	**0,42**	69,6
COP14	0,00	**1,49**	37,3
COP16	0,15	**0,86**	68,3

Table 5
Click here to download Table: Table 5.doc

Table 2. Polar compounds detected in coprolites as an TMS derivatives. Abundances normalized to $C_{16:0}$ fatty acid, the most abundant lipid.

Compound	M+	COP09	COP06	COP05	COP14	COP16	COP18
Octanoic acid-TMS	216	2	3	3	2	3	4
Urea- bis-TMS	204	2	5	4	4	1	1
Benzoic acid-TMS	194	5	7	7	6	8	11
Nonanoic acid-TMS	230	9	10	10	6	8	11
Decanoic acid-TMS	244	6	10	11	12	12	13
1-Dodecanol-TMS	258	10	3	5	6	3	11
1-Tridecanol-TMS	314	4	2	3	3	1	3
1-Tetradecanol-TMS	328	15	8	14	10	8	14
Tetradecan-1-ol?	214	32	12	14	13	13	53
Levoglucosan-TMS	378	2	2	2	1	1	0
Tridecanoic acid-TMS	286	2	1	4	2	2	4
1,4-Benzenedicarboxylic acid-TMS	310	16	8	8	14	19	25
1-Hexadecanol-TMS	314	57	44	45	36	69	54
Pentadecanoic acid-TMS	314	9	10	10	10	10	11
9H-Fluoren-9-one	180	8	3	4	4	3	4
Hexadecanoic acid-TMS	328	**100**	**100**	**100**	**100**	**100**	**100**
Octadec-9Z-enol-TMS	340	68	37	44	24	77	89
1-Octadecanol-TMS	342	77	40	52	42	83	80
2,6,10,14-tetramethylpentadecanoic acid (pristanic acid)-TMS	370	3	4	3	3	2	3
3,7,11,15-tetramethylhexadecanoic acid (phytanic acid)-TMS	384	2	2	2	2	1	2
Trans-9-Octadecenoic acid-TMS	354	14	7	9	9	16	16
Octadecanoic acid-TMS	356	33	32	34	29	34	38
1-Eicosanol-TMS	370	7	5	5	5	5	5
Unknown C18-Unsaturated Fatty Acid	354	9	7	8	8	11	11
1-Docosanol-TMS	398	17	14	14	16	14	22
Heneicosanoic acid-TMS	398	3	2	3	2	2	2
2-Palmitin-TMS	474	7	8	5	7	11	14
1-Palmitin-TMS	474	20	12	14	16	21	23
Docosanoic acid-TMS	412	19	17	17	17	19	18

Tetracosanol-TMS	424	4	3	3	3	3	4
2-Stearin	502	7	5	4	4	9	15
1-Stearin	502	17	10	12	11	18	25
Tetracosanoic acid-TMS	440	7	7	7	7	7	6
1-Hexacosanol-TMS	452	4	3	2	0	5	2
Pentacosanoic acid-TMS	454	4	4	4	4	5	4
1-Heptacosanol-TMS	466	5	5	2	3	6	0
Hexacosanoic acid-TMS	468	5	6	4	5	5	8
1-Octacosanol-TMS	480	39	31	32	28	30	33
1-Nonacosanol-TMS	494	2	2	2	1	2	2
Octacosanoic acid-TMS	496	18	15	14	12	12	15
Cholesterol-TMS	458	14	15	21	18	17	14
1-Triacontanol-TMS	508	23	19	21	18	19	18
Campesterol-TMS?	472	7	9	6	5	7	7
Stigmasterol-TMS?	484	2	1	2	1	2	1
Triacontanoic acid-TMS	524	9	7	9	5	6	6
Sitosterol-TMS	486	55	46	45	39	57	52
1-Dotriacontanol-TMS	536	7	0	5	0	0	6
Cholesta-3,5-dien-7-one	382	6	5	3	5	5	6
beta-Amyrin-TMS?	498	5	3	3	4	3	2
alpha-Amyrin-TMS?	498	4	4	4	4	6	4
alpha-Amyrone	424	3	3	4	5	5	4
Stigmasta-3,5-dien-7-one	410	10	9	9	16	19	18